

Real-Time Scheduling for Time-Sensitive Networking: A Systematic Review and Experimental Study

Chuanyu Xue[†], Tianyu Zhang[†], Yuanbin Zhou[‡], Song Han[†]

[†]Dept. of Computer Science and Engineering, University of Connecticut

[†]Email: {chuanyu.xue, tianyu.zhang, song.han}@uconn.edu

[‡]TTTech Auto AG

[‡]Email: yuanbin.zhou@tttech-auto.com

Abstract—Time-Sensitive Networking (TSN) has been recognized as one of the key enabling technologies for Industry 4.0 and has been deployed in many time- and mission-critical industrial applications, e.g., automotive and aerospace systems. Given the stringent real-time communication requirements raised by these applications, the Time-Aware Shaper (TAS) draws special attention among the many traffic shapers developed for TSN, due to its ability to achieve deterministic latency guarantees. Extensive efforts on the designs of scheduling methods for TAS shapers have been reported in recent years to improve the system schedulability, each with their own distinct focuses and concerns. However, these scheduling methods have yet to be thoroughly evaluated, especially through experimental comparisons, to provide a systematical understanding on their performance using different evaluation metrics in various application scenarios. In this paper, we fill this gap by presenting a comprehensive experimental study on the existing TAS-based scheduling methods for TSN. We first categorize the system models employed in these work along with their formulated problems, and outline the fundamental considerations in the designs of TAS-based scheduling methods. We then perform extensive evaluation on 16 representative solutions and compare their performance under both synthetic scenarios and real-life industrial use cases. Through these experimental studies, we identify the limitations of individual scheduling methods and highlight several important findings. This work will provide foundational knowledge for the future studies on TSN real-time scheduling problems, and serve as the performance benchmarking for scheduling method development in TSN.

Index Terms—Time-sensitive networking (TSN), real-time scheduling, time-aware shaper (TAS), experimental study

I. INTRODUCTION

Time-Sensitive Networking (TSN), as an enhancement of Ethernet, is being recognized as the next-generation local area network (LAN) technology to support the co-existence of information technology (IT) and operation technology (OT) in the industrial Internet-of-Things (IIoT) paradigm. TSN targets at providing deterministic end-to-end communications between Layer-2 networks which is highly desirable for many real-time industrial applications, e.g., process automation and factory automation [1], [2]. To enable such deterministic network communications, the TSN Task Group has developed a suite of traffic shapers in the TSN standards, including Credit-Based Shaper (CBS) [3], Asynchronous Traffic Shaper (ATS) [4], Peristaltic Shaper (PS) [5] and Time-Aware Shaper (TAS) [6], to handle different traffic types and satisfy real-time communication requirements. In terms of providing strict real-

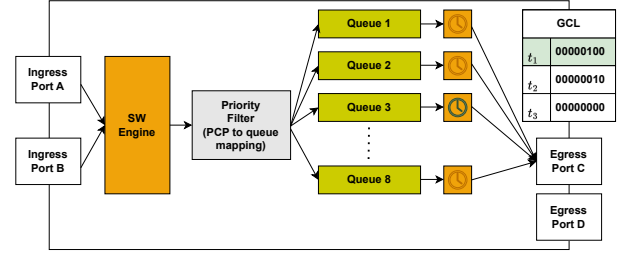


Fig. 1. An illustration of TAS mechanism in a TSN bridge.

time performance guarantees, TAS stands out by leveraging network-wide synchronization and time-triggered scheduling mechanisms [7], [8], making it an enabling feature to support ultra-low-latency traffic in industrial applications.

TAS operates in a time-triggered scheduling fashion similar to TTEthernet [9], and it achieves deterministic communications by buffering and releasing traffic at specific time instances following a predetermined schedule. Specifically, as shown in Fig. 1, each egress port in a TSN bridge is equipped with a set of time-gated queues for buffering frames from each traffic. A scheduled gate mechanism is utilized to open or close individual queues and control the transmission of frames according to a predefined Gate Control List (GCL). Each GCL includes a limited number of entries, each of which provides the status of associated queues over a particular duration. The network-wide schedule is generated by the Centralized Network Configuration (CNC) and deployed on individual TSN bridge. The priority filter utilizes a 3-bit Priority Code Point (PCP) field in the packet header to identify the stream priority, and direct incoming traffic to the appropriate egress queue according to the priority-to-queue mapping. It is worth noting that this mapping may vary across different bridges, making the same traffic be assigned to different queues on the bridges along its routing path.

Although the scheduling mechanism of TAS is clearly defined in the IEEE 802.1Qbv standard, the configuration of TAS, e.g., the generation of GCL and the queue assignment for individual traffic at each hop, needs significant research to improve the performance of TAS in terms of system schedulability, network throughput, and system reliability, etc. Specifically, the fundamental question underlying the TAS-based real-time scheduling in TSN is how to generate a network-wide schedule to guarantee the timing requirements of all

time-triggered (TT) traffic [10], [11]. Given that the industrial applications that employ TAS-based TSN as the communication fabric can be diverse from many different perspectives (e.g., traffic patterns, QoS requirements, network topology, and deployment environments), the specific scheduling problems to be studied may vary significantly. This results in a large amount of research efforts from researchers and practitioners to study various system models and develop corresponding methods to address specific TAS-based scheduling problems. These studies considerably enrich the TSN literature, paving the way for improved network performance in TSN.

There are several recent work reviewing the existing literature on real-time scheduling in TSN networks (e.g., [8], [11]–[15]). These studies provide a comprehensive survey and a broad overview of the TSN standards, identifying the limitations of the existing TSN scheduling methods and outlining future research directions to address these limitations. In addition, [11], [16] provide rigorous comparisons among various TSN scheduling approaches, with [11] primarily focusing on TAS-based studies and [16] extending the comparison to all TSN shapers. However, all the work mentioned above are either on a review basis or only perform conceptual comparison among the existing solutions, which are not sufficient to provide a thorough performance evaluation to determine the effectiveness of individual methods.

To fill this gap, this paper presents comprehensive experiment designs and quantitative performance comparison among 16 time-triggered scheduling methods proposed for TSN since 2016 (i.e., [17]–[31]). We conducted a thorough experimental study by considering eight key characteristics of the dataset – including system utilization, number of streams, periodicity pattern, payload size, deadline, network scale, available queues, and line rate – in both synthetic scenarios and real-life use cases in aerospace and automation industries. Furthermore, we conducted a detailed analysis for the impact of the aforementioned settings on the performance of the scheduling methods, applying six important metrics including feasibility, scalability, GCL length, link utilization, queue utilization, and end-to-end delay. Our study shows that there is no one-size-fits-all solution, as no single method outperforms others in all scenarios. Furthermore, we demonstrate that diverse workload and network settings significantly complicate the fair evaluation of scheduling methods without introducing bias. Our findings can help the community understand the benefits and drawbacks of existing TSN scheduling methods and provide valuable insights for the development of future TSN scheduling methods.

In summary, this work makes the following contributions:

- 1) We provide a comprehensive up-to-date review of TAS-based TSN real-time scheduling methods for TSN, and outline the fundamental considerations in the designs of TAS-based scheduling methods.
- 2) We identify the key parameter settings in practical TSN networks (e.g., the processing delay and synchronization error) through the measurement results collected from a real-life TSN testbed.
- 3) We perform extensive evaluation on 16 representative TAS-based scheduling methods, comparing their performance using metrics that are of interests to the industry, in comprehensive synthetic scenarios.
- 4) We summarize the findings from our performance evaluation, including the limitations identified from individual scheduling methods, as well as important observations that can provide insights for future research on TSN real-time scheduling method design.

The remainder of this paper is structured as follows. Section II presents the fundamental concepts and system models used in the literature for real-time scheduling in TSN. Section III provides a classification of existing scheduling methods and introduces the key ideas underlying their algorithms. Section IV describes our experimental settings. Section V presents the experimental results and discusses the significant findings from our study. Finally, Section VI concludes the paper and discuss the future work.

II. BACKGROUND AND SYSTEM MODEL

This section presents an overview of the network model, traffic models, and scheduling models for real-time traffic scheduling in TSN. It provides the foundation for the discussion of the TAS-based scheduling methods in Section III.

A. Network Model

A TSN network consists of two types of devices: bridges and end stations (ES). A bridge can forward Ethernet frames for one or multiple TSN streams according to a schedule constructed based on IEEE 802.1Q standard. Each ES is either a *talker*, acting as the source of TSN stream(s), or a *listener*, acting as the destination of TSN stream(s).

Each full-duplex physical link connecting two TSN devices (either bridge or ES) is modeled as two directed logical links. Each logical link is associated with the following four attributes, which are determined by the capacity of the bridge or ES connected by the link:

- **Propagation delay** refers to the time duration of a signal transmitting on the physical link (i.e., Ethernet cable). This delay is solely dependent on the length of the cable and the type of physical media used.
- **Line rate** refers to the data rate that frames can be transmitted over a logical link within a given time interval. There are three line rates widely employed for TSN (10/100/1000 Mbps), while higher-speed TSN bridges with 10/100Gbps line rates are also developed recently [32].
- **Number of egress queues** refers to the available egress queues used by TT traffic. The IEEE 802.1Q standard sets a max of eight queues per egress port of a TSN bridge [33].
- **Maximum number of GCL length** of a logical link is set between 8 and 1024 for typical TSN bridges [18].

In addition to the attributes associated with logical links, TSN networks also have a network-wide attribute that is shared across all nodes and links such as the synchronization error:

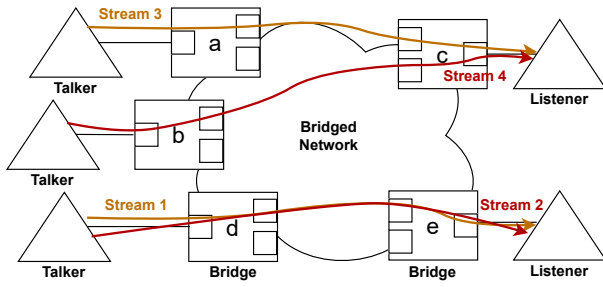


Fig. 2. An example TSN network comprising 5 bridges and 5 end stations (ES) with 4 streams deployed in the network.

- **Synchronization error** is defined as the maximum time offset between any two logical clocks in the network.

In TSN networks, a stream refers to an unidirectional flow of data transmitted from a single talker to one or multiple listeners, passing through bridges over multiple logical links. For example, in Fig. 2, there are four streams transmitting in a TSN network that comprises 5 bridges and 5 ESs. As one of the key enabling features, TSN supports the co-existence of differentiated services and applications, through the modeling of various types of streams including best-effort (BE) traffic, audio and video (AVB) traffic, and time-triggered (TT) traffic, also known as scheduled traffic. Driven by the ultra-low latency requirements posed by real-time industrial applications, the literature mainly focuses on the TT traffic scheduling problems, which is the emphasis of this paper.

B. Traffic Models

Each TSN stream can be characterized by five parameters: release time, period, payload size, deadline, and jitter. Each of these parameters can be modeled individually in order to capture the specific characteristics of the targeted traffic type, based on the application scenario under study.

- **Release time:** the release time of a stream is defined as the time instance when its first frame is injected into the TSN network by the talker. Depending on whether the talker is able to determine the release time of its stream(s), the traffic model can be classified into fully schedulable traffic and partially schedulable traffic. The fully schedulable traffic model allows the scheduler to configure the release time of each stream and thus yield higher schedulability. It, however, will incur increased scheduling complexity compared to the partially schedulable traffic model.
- **Period:** The period of a stream determines the inter-arrival pattern of its frames. It can be classified into strictly periodic and non-strictly periodic models based on the determinism of their arrival times. In a strictly periodic model, each frame follows the same release offset, resulting in a fixed time interval between any two consecutive frames when they arrive at the egress of the talker. By contrast, in the non-strictly periodic model, frames from the same stream can be released with varied but bounded offsets.

- **Payload size:** Payload size refers to the size of the application data to be transmitted within a stream, which may comprise multiple frames during each period when the payload size is larger than 1500 bytes¹. There are two main strategies to transmit multiple frames from the same stream in each of its period. The first approach schedules each frame individually while preserving the frame order of the same stream by introducing additional constraints. By contrast, the second approach schedules all frames from the same stream successively within an extended time duration on each link.

- **Deadline:** The deadline of a stream defines the time by which the stream must be received at the listener, such that the release time plus the end-to-end delay does not exceed this deadline. The deadline of a stream can be modeled as implicit (equal to the period), constrained (less than the period), or arbitrary, according to the application scenario. Note that, under the arbitrary deadline model, a frame released in its period can be scheduled into the next period interval and such case should be carefully handled in the scheduling method to avoid potential conflicts.

- **Jitter:** The jitter captures the variation in end-to-end stream delay (i.e., the difference between the minimum and maximum delays of frame transmissions from the same stream), following the definition in IEC/IEEE 60802 TSN Profile [34]. The zero-jitter model enforces fully deterministic traffic behavior for each frame, while the jitter-allowed model permits limited conflicts from other traffic on delay, subject to a user-defined jitter upper bound. Fig.3(a) illustrates a jitter-allowed scheduling example for stream S1, with a delay of 6 for the first instance and 12 for the second. Fig.3(b) demonstrates how jitter arises from interference when both S1 and S2 share a GCL entry along the path, resulting in a bounded delay between 10 and 12.

C. Scheduling Models

Based on the described network and task models, the TAS-based real-time scheduling problems in TSN aim to construct feasible communication schedules (assignment of transmission times for each stream on involved bridges) to satisfy the temporal constraints imposed by the streams deployed in the TSN network. For this aim, a range of scheduling models have been proposed to define the constraints made on end-to-end delay, jitter, queuing assignment, fragmentation and routing path, according to specific requirements in the target scenarios. In this section, we summarize these scheduling models and categorize them according to their unique features.

- **Models based on Queuing Delay:** The end-to-end delay of a stream is defined as the duration between the time when the frame is released on talker and the time when the entire frame is received by the listener. This delay consists of four parts: processing delay, propagation delay, transmission delay, and queuing delay. In TSN, the propagation and processing delays

¹According to the IEEE 802.1Q standard, the maximum frame size is 1522 bytes, including a frame payload and a 22-byte frame header containing the VLAN Tag, Ethernet header, and FCS.

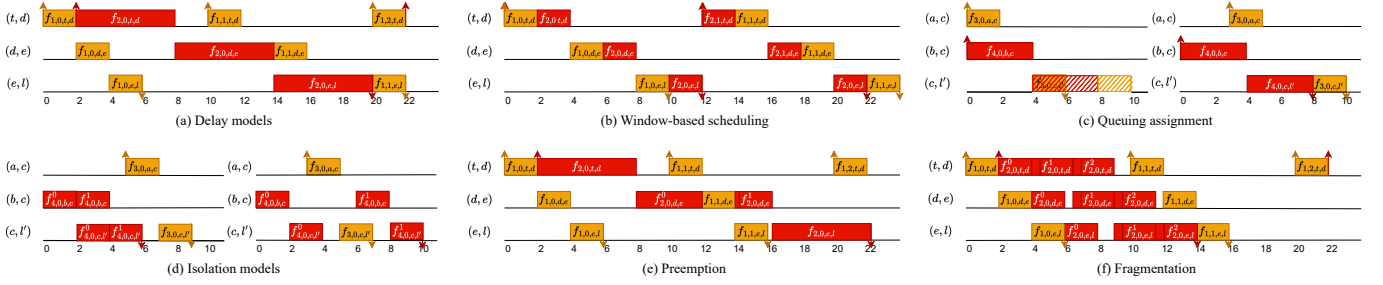


Fig. 3. An illustration of various scheduling models applied on Fig. 2, where $f_{i,k,a,b}$ indicates the k -th frame of stream- i scheduled on link (a,b) . Up arrow indicates the frame release time at the talker and down arrow indicates the frame reception time at the listener. Solid area indicates the actual transmission pattern and shallow area indicates the traffic planning result.

are typically considered constant [23]. The transmission delay depends on the payload size and the line rate of the link. The queuing delay refers to the amount of time that a frame spends in the queue. Based on the assumption on the queuing delay, the scheduling models can be classified as no-wait and wait-based models. No-wait scheduling model requires consecutive frame transmissions along the path, i.e., frames should be forwarded without queuing delay. As a result, no-wait scheduling model solely focuses on planning the release times of the streams on the talkers, which typically results in reduced scheduling effort but smaller solution spaces. On the other hand, wait-based scheduling model is more general since it allows frames to be stored in the queue and forwarded at a later time, therefore significantly enlarge the solution space. For example, Fig. 3(a) follows the wait-based scheduling model as the second instance of stream S1 waits 2 time units on link (d,e) and 4 time units on link (e,l) . The no-wait scheduling model cannot find a feasible solution in this case.

• **Models based on Scheduling Entity:** The scheduling models can be classified into frame-based, window-based and class-based models depending on the objects used in the scheduling methods for the allocation of GCL entry [8]. The frame-based model schedules the transmission time of each frame in a per-stream fashion and directly maps it to a dedicated GCL entry. By constraining that no overlap exists for any two frames' transmission time, the frame-based model guarantees that there is no interference between any two streams. The window-based model partitions frames into different groups and jointly schedules the transmission time of each group. As each GCL entry is shared by a group of frames, the transmission order of each frame can be interfered by other frames within the group and results in jitter. For example, in Fig. 3(b), stream S1 and S2 are assigned into the same egress queue and share the same GCL entry according to a window-based scheduling model. Their transmission orders in two consecutive periods are different within the window which causes jitter. It is worth noting that in window-based scheduling models, the large inter-dependencies between window allocation and traffic grouping may pose significant runtime and memory overhead [29]. The class-based scheduling model allocates resources for each traffic class and guarantees the same deadline and jitter requirements

for a whole class. Each traffic class is mapped to a dedicated egress queue. Since the class-based model is mainly applied for asynchronous traffic class such as AVB and BE traffic, it is out of the scope of this paper [35].

• **Models based on Queuing Assignment (QA):** Based on how the frames are assigned to the egress queue(s), the scheduling models can be classified into unrestricted QA models and explicit QA models. The unrestricted QA model is derived from the TTEthernet scheduling method, which assumes a global schedule that defines the temporal behavior of all frames without considering queuing. However, implicit QA model is not directly applicable to TSN, as neglecting QA can result in deviations in actual transmission time from the designed schedule due to FIFO property violations. For instance, as shown in Fig. 3(c), the schedule on the left is valid under the unrestricted QA model where two streams are forwarded simultaneously at their first hop. Stream S4 is scheduled earlier than S3 on link (c,l') without any conflicts. However, if both streams are assigned to the same queue, the frame of S3 will use transmission slot allocated to S4 during run time, causing S4 to be suspended and miss its deadline. Please note that this inconsistency can only happen under the wait-allowed model, since the no-wait model forwards frames immediately without any queuing.

To avoid the schedule inconsistency, explicit QA models jointly compute the queuing assignment along with the schedule to isolate streams into different queues. For this aim, several isolation constraints are proposed which can be categorized into three levels: FIFO, frame-based, and stream-based isolation. The basic idea of the FIFO isolation is to prevent reordering forwarding sequence when they are assigned to the same queue. For instance, in Fig. 3(c), the schedule on the right side enforces stream S4 to arrive earlier than S3, so that the forwarding order matches the predefined schedule, even if they are within the same queue.

Frame-based isolation and stream-based isolation are comparatively more realistic as they take into account frame loss, unbounded processing jitter, and interleaving caused by fragmentation when the payload size is larger than the MTU. For example, as shown in Fig. 3(c), stream S3 can replace S4 if the frame of S3 is lost on link (c,l') or the arriving order is altered due to physical jitter. The key idea of frame-based

isolation is to ensure that at one time, only one frame can exist in the queue so that one frame is not interfered by another frame's fault condition. Specifically, it ensures that any two frames cannot co-exist in the same queue, as illustrated on the right side of Fig. 3(d). The frame of stream S3 can only arrive at link (c, l') after the first segment of stream S4 is dispatched. The second segment of S4 can only arrive at link (c, l') after the frame of S3 is dispatched. Compared to frame-based isolation, stream-based isolation is more stringent, where the frame of the current stream can only be enqueued after all frames of the previous stream have been fully dispatched, as shown on the left side of Fig. 3(d). The frame of S3 must wait until all the segments of S4 are dispatched. It is suggested that the frame-based isolation provides more flexibility, but it takes more time to solve compared to the stream-based model [17].

- **Models based on Routing and Scheduling Co-Design:**

Scheduling models can be further categorized as fixed routing and scheduling (FRS) models or joint routing and scheduling (JRS) models. The JRS models allows the co-design of route selection and schedule construction, while the FRS models focus on the schedule construction, assuming that the routes are pre-determined. By optimizing the routing and scheduling decisions in a joint fashion, the JRS models offer better resource utilization and schedulability in general when compared to the FRS models. However, they typically incur much higher computational overheads and may not be able to find feasible solutions if the computing resource is constrained.

- **Models based on Fragmentation:** In the context of IEEE 802.1Qbv standard, fragmentation occurs when a frame is split into smaller pieces to fit the MTU size of a network. However, default fragmentation can result in high latency due to the large frame size. To address this issue, joint fragmentation and scheduling (JFS) model has been proposed, which determines the number and size of fragments along with the schedule construction. The JFS model to some extent can improve schedulability, especially in cases when a deadline is exceeded, even in the absence of queuing delays. Fragmenting a large frame into multiple segments reduces transmission delay, as segments are transmitted separately, eliminating the need to wait for the entire frame to be fully received before the forwarding process. For example, if we consider stream S2 in Fig. 3(f) with a transmission duration 6 time units less than the MTU, the minimum end-to-end delay for the stream to travel through the three hops is 18 time units. However, if we fragment the frame into three segments, forwarding can start after the first segment is received on each hop. In this scenario, if the deadline is set to 12, S2 can only be scheduled for transmission under the JFS model. It is important to note that segments carry the entire header size, which may post negative impact on the link utilization.

- **Models based on Preemption:** IEEE 802.1Qbu standard delineates frame preemption as the capacity of an express frame to interrupt the transmission of a preemptable frame and subsequently resume the preempted frame at the earliest available opportunity. Frames may be assigned distinct pre-

emption classes at different hops, with only express frames being able to interrupt preemptable frames. For instance, in Fig. 3(e), the frame of stream S2 on link (d, e) is designated as a preemptable class, and is consequently preempted by the frame of S1, classified as an express class, at time 12 during the transmission. Following the completion of stream S1's transmission, stream S2 resumes its transmission. It is worth noting that joint preemption and scheduling (JPS) do not reduce transmission delay compared to JRS, as frames can only be forwarded after all segments are fully received and reassembled. For example, in Fig. 3(e), link (e, l) cannot forward at time 12 when the first fragment is received but can only proceed after time 16 when both fragments have been received. Nonetheless, if preemption was disabled, S1 would fail to meet its deadline, resulting in an unschedulable stream set. In addition, as fragmentation only occurs when necessary, preemption offers better bandwidth conservation when compared to the JFS model due to the reduced number of generated headers. For example, there is merely one additional header created for the second fragment of the frame of S2 along its path in Fig. 3(e). By contrast, a total number of six headers are generated under the JFS model in Fig. 3(f).

III. REAL-TIME SCHEDULING METHODS FOR TSN

This section provides a comprehensive review of 16 representative TAS-based real-time scheduling methods in TSN by categorizing them based on their employed system models and proposed scheduling methods (see Fig. 4). Specifically, we first classify all the work into FRS or JRS methods based on whether the routing paths of individual streams are pre-determined or jointly selected when constructing the communication schedule. The work in each group is then further divided into no-wait and wait-allowed methods based on the employed delay model depending on if the frames can wait in bridges' egress queue or not. Finally, we categorize each work into exact or heuristic solutions based on if the method can yield optimal schedule or not. Please note that some work proposes both exact and heuristic solutions, while in this paper we only evaluate one of them based on their key ideas to make the survey more concise and informative.

A. Fixed Routing and Scheduling (FRS) Methods

FRS methods assume that the routing paths of individual streams are pre-determined as the input of the scheduling algorithms. Based on the IEEE 802.1Qca standard, the default routing paths generated by the Shortest Path Bridging Protocol ensure that all streams are routed along their shortest paths between the talkers and listeners [36].

- 1) *No-wait*: No-wait scheduling model requires that frames are forwarded along its routing path without queuing delay. Among the 16 real-time scheduling methods that we are examining in this paper, five methods employ a combination of the FRS and no-wait models. They focus on minimizing the end-to-end latency based on the predetermined routing.

- **SMT-NW:** Durr et al. [23] address the crucial problem of reducing end-to-end latency of TT traffic and increasing

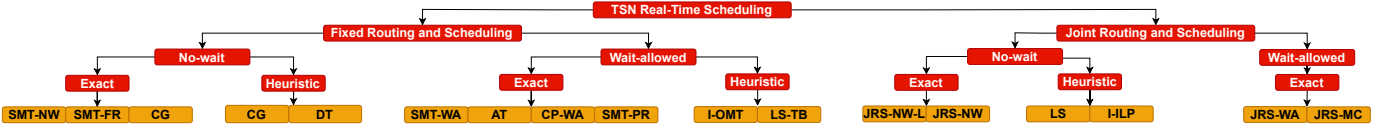


Fig. 4. Classification of TSN scheduling algorithms based on the system model and scheduling approaches implemented in our evaluation.

$$\begin{aligned}
 &\forall f_{i,k}, f_{j,l} \in F : \forall (a,b) \in \text{Path}(i) \cap \text{Path}(k) : & \forall f_{i,k}, f_{j,l} \in F : \forall (a,b) \in \text{Path}(i) \cap \text{Path}(k) : & \forall (a,b) \in E : \\
 &\text{start}_{i,k,a,b} - \text{end}_{j,l,a,b} \geq -M * (1 - x_{i,j,k,l,a,b}) & (\text{start}_{i,k,a,b} - \text{end}_{j,l,a,b} \geq 0) & A = \{[\text{start}_{i,k}, \text{end}_{i,k,a,b}] : (a,b) \in \text{Path}(i)\} : \\
 &\text{start}_{j,l,a,b} - \text{end}_{i,k,a,b} \geq -M * (x_{i,j,k,l,a,b}) & (\text{start}_{j,l,a,b} - \text{end}_{i,k,a,b} \geq 0) & \text{AllDifferent}(A) \\
 \text{(a): Big-M formalization in ILP} & & \text{(b): Logical formalization in SMT} & \text{(c): All-different formalization in CP}
 \end{aligned}$$

Fig. 5. An example of different formalization approaches for no-overlap constraints.

available bandwidth for BE traffic. The key idea is to adapt this problem to the no-wait job-shop scheduling problem [37]. They propose an exact solution using the CPLEX Integer Linear Programming (ILP) solver with Big-M logical expressions as shown in Fig. 5(a) and a compression algorithm in post-processing that minimizes the guard bands to save bandwidth. To tackle the scalability issue, a heuristic approach based on Tabu search is also proposed.

- **CG:** Falk et al. [31] tackle the critical issue of slow solving process in existing FRS and no-wait based methods. Their approach constructs a conflict graph to capture the collision between individual stream's transmission time, and thus accelerate the solving process. The key idea is to identify an independent set within this graph and gradually expand it to obtain a valid schedule. Based on the search state, their solution automatically selects between a quick algorithm or ILP solver, strategically combining heuristic and exact methods.
- **SMT-FR:** Jin et al. [26] address the problem of enhancing schedulability in a no-wait scheduling approach, by introducing a framework for joint scheduling with fragmentation. The key idea is to simultaneously determine the number and size of fragments, along with schedule generation. The problem is formalized using a Satisfiability Modulo Theories (SMT) formulation, as presented in Fig.5(b), and is solved using the Z3 solver. To address the scalability issue, the authors also propose a heuristic solution based on fixed priority scheduling.
- **DT:** Zhang et al. [38] addresses the large runtime issue associated with traditional scheduling processes. They propose a stream-aware model conversion that accelerates the scheduling process for zero-jitter models. It employs the divisibility theory to detect collision and speed up this process by only comparing the first instances of two streams. In addition, they introduce an efficient incremental list scheduler without traceback, further reducing the runtime.

2) *Wait-allowed:* In the wait-allowed scheduling model, frames can be stored in the queue and forwarded at a later time. It thus has a larger solution space compared with that of the no-wait scheduling model. We evaluate the following six works that employ a combination of FRS and wait-allowed models to solve the real-time scheduling problems in TSN.

- **SMT-WA:** Craciunas et al. [17] focus on accurately modeling the behavior of TAS-based scheduling mechanism. They formalize the constraints for creating valid offline schedules using a SMT formulation for wait-allowed scheduling problems, resolved with the Z3 solver. To ensure correctness, a key aspect of their work is the introduction of queuing isolation models such as frame- and stream-based isolation.
- **AT:** Oliver et al. [18] address the challenge that GCLs only support a limited number of entries in practical implementation. Their study introduces a window-based scheduling method that applies array theory in an SMT solver, taking the maximum number of GCL entries as the algorithm input. In addition, this work incorporates queuing assignment and isolation models into the solution.
- **I-OMT:** Jin et al. [29] also address the practical limitation of GCL length. Instead of setting hard constraint on the GCL length, it minimizes the GCL length by proposing an iterative-Optimization Modulo Theories (OMT)-based approach to scheduling streams by group. The queuing assignment is calculated for each stream based on its data size, shortest routing path, and deadline, and taken as the input of the iterative-OMT solver. The stream-based isolation is formulated as a constraint to guarantee the correctness of queuing assignment.
- **CP-WA:** Vlk et al. [28] focus on modeling deterministic TT traffic communications in TSN through constraint programming (CP) formalization. As shown in Fig.5(c), CP provides a more efficient solution to scheduling problems with an all-different constraint compared to other formalizations such as SMT and ILP. The study also proposes a decomposition optimization proposed to enhance scalability, which alternates between routing and scheduling searches.
- **SMT-PR:** Zhou et al. [30] aim to enhance schedulability by integrating the preemption feature from the IEEE 802.1Qbu standard [39]. The key idea is an SMT-based approach to assigning streams to express and preemptable classes while jointly determining the schedule. The allowed maximum number of preempted segments is taken as the algorithm input.
- **LS-TB:** Vlk et al. [24] address the challenge of poor scalability in scheduling large-scale TT traffic, an inherent problem when using general third-party solvers. Their scheduler can revert to a previous search stage and modify the timing and

queuing assignment if the current frame conflicts with any other scheduled frames. The authors utilize two data structures, the global and local conflict sets, to decide the search order.

B. Joint Routing and Scheduling (JRS) Methods

A feasible schedule may not be found when the routing paths of the streams are given under the FRS model. By contrast, the JRS-based methods allow the scheduler to decide the routes and schedules in a joint fashion for individual streams, thus open up opportunities to offer better network resource utilization and schedulability.

1) *No-wait*: The following work study the TSN scheduling problems using a combination of JRS and no-wait models.

- **JRS-NW-L**: Falk et al. [21] propose an ILP-based approach to determining the routing path of each stream and the schedule of the stream set. In contrast to using the Big-M formulation commonly employed by other ILP-based models (e.g., [19], [21]–[23]), the authors opted for indicator constraints to address the logical constraints.
- **JRS-NW**: Hellmanns et al. [20] tackle the high computational complexity in solving JRS-based scheduling. They first evaluate the impact of workload and network topology on the performance, and then present a runtime optimization framework for JRS and no-wait scheduling, including input and model generation optimization, and solver parameter tuning.
- **LS**: Pahlevan et al. [25] address the inherent slow scheduling process in JRS-based scheduling methods. Their heuristic-based list scheduling algorithm searches all potential release times on a route, and only moves to the next when no available release time remains on the current route. The search order is governed by the hops of each flow's shortest path. Notably, this algorithm has no backtracking mechanism, thereby it returns infeasible once the algorithm traverses all paths of one flow without finding a solution.
- **I-ILP**: Atallah et al. [27] aim to design an efficient method for computing no-wait schedules and multicast routing in large-scale TSNs. The key idea is a three-part solution: iterative-ILP based scheduling for enhanced scalability, Degree of Conflict (DoC)-aware partitioning to group streams, and the DoC-aware multipath routing (DAMR) technique. Together, they form a comprehensive solution to solve the JRS problem.

2) *Wait-allowed*: There are two works that study the real-time scheduling problems in TSN using a combination of JRS and wait-allowed models. We summarize them below.

- **JRS-WA**: Schweißguth et al. [19] address the issue that existing methods may exclude feasible solutions due to disregard of routing in their design space. It proposes an ILP-based approach to jointly determining the routing path and scheduling. In addition, the authors enhance the search speed by excluding infeasible routing paths during pre-processing, reducing the scheduling complexity without sacrificing schedulability.
- **JRS-MC**: Schweißguth et al. [22] extend the ILP-based JRS scheduling approach to incorporate multicast traffic streams. They argue that including multicast features requires more than a trivial extension from the unicast model, necessitating

additional scheduling constraints to prevent loops and negative latency. The authors investigate various objectives, examining schedule quality improvements and trade-offs between quality and runtime. They also introduce optimizations for pre-processing and model generation, demonstrating that these enhancements significantly reduce the solver's runtime.

C. Scheduling Methods with Other Considerations

The scheduling methods that we summarized in Section III-A and Section III-B focus on finding a feasible network-wide configuration, including routing paths and schedules, to meet the end-to-end timing requirements of a given set of streams. In addition to this fundamental feasibility requirement, there are several other important optimization objectives considered in the literature. Due to the page limit, we do not include them in the evaluation but summarize them below for the completeness of the discussion.

Delay and jitter. Minimizing the end-to-end delay of the streams is one of the most critical design objectives of the TSN schedulers [40], [41]. Scheduling methods based on the no-wait model (e.g., [20], [21], [23], [25]–[27], [31]) reduce the end-to-end delay by eliminating the queuing delay at each TSN bridge. On the other hand, [19], [22] achieve this objective by incorporating additional objective functions (e.g., minimize the average delay among streams), and [26] leverages stream fragmentation to reduce the transmission delay by allowing more parallel transmissions. The experienced maximum jitter is another critical metric to evaluate the performance of TSN-based applications [42]. In [18], the authors minimize the maximum jitter of TSN streams by controlling the window size.

Number of queues. Minimizing the number of queues used per hop is another important design objective. Since TT traffic must have exclusive queue access to ensure determinism, it is crucial to limit the number of utilized queues, reserving available ones for other traffic classes such as AVB and BE. As discussed in Section II-C, no-wait based scheduling utilizes only one queue [20], [21], [23], [25]–[27], [31]. Furthermore, wait-allowed based scheduling can incorporate an additional objective function to minimize the queue usage [17], [28].

Co-existence. In addition to the TT traffic, some other traffic types (e.g., AVB and BE traffic) can co-exist in the same TSN network and share the network resource with the TT traffic. Some research work investigated how to enhance the performance of the non-TT traffic while guaranteeing the real-time performance of the TT traffic. For instance, Durr et al. [23] proposed a schedule compression technique to reduce the number of guard bands and improve the throughput of other traffic. Houtan et al. [43] introduced a set of optimization functions to enhance the QoS for the BE traffic by adjusting the temporal distribution of the schedule.

Reliability. Ensuring reliable frame transmissions is crucial for TSN. Reusch et al. [44] proposed a dependability-aware JRS framework that uses redundant disjoint message routes to tolerate link failures. Zhou et al. [45] proposed an ASIL-decomposition-based JRS framework that addresses systematic

TABLE I
A SUMMARY OF SYSTEM MODELS AND SCHEDULING APPROACHES FOR CONSIDERED TSN SCHEDULING METHODS.

Article	Fully schedulable	Strictly periodic	No-wait	Window-based	Queueing	Routing	Multicast	Heuristic	Exact	Algorithms	Enhancements
Craciunas et al. (SMT-WA)	✓	✓			✓				✓	SMT	
Dürr et al. (SMT-NW)	✓	✓	✓					(✓)	✓	ILP (Tabu)	
Schweissguth et al. (JRS-WA)	✓	✓				✓			✓	ILP	Paths reduce
Oliver et al. (AT)	✓			✓	✓				✓	SMT	Array-theory
Falk et al. (JRS-NW-L)	✓	✓	✓			✓			✓	ILP	Logic indicator
Pahlevan et al. (LS)	✓	✓	✓			✓		✓		List scheduler	
Schweissguth et al. (JRS-MC)	✓	✓				✓	✓		✓	ILP	Paths reduce
Atallah et al. (I-ILP)	✓	✓	✓			✓	✓	✓		Iterative-ILP	
Xi et al. (I-OMT)				✓	✓			✓	(✓)	Iterative-OMT	
Falk et al. (CG)	✓	✓	✓			✓		✓	✓	Conflict-graph	
Hellmanns et al. (JRS-NW)	✓	✓	✓			✓			✓	ILP	Path cut-off
Jin et al. (SMT-FR)	✓	✓	✓					(✓)	✓	SMT (WCRT)	Fragmentation
Vlk et al. (CP-WA)	✓	✓			✓			(✓)	✓	CP (Decompose)	
Vlk et al. (LS-TB)		✓			✓			✓	(✓)	List scheduler	Traceback
Zhou et al. (SMT-PR)	✓								✓	SMT	Preemption
Zhang et al. (DT)	✓	✓	✓					✓	(✓)	Divisibility	

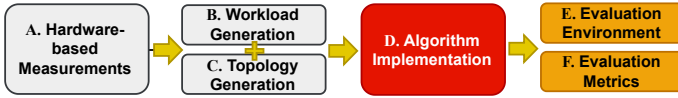


Fig. 6. An overview of the evaluation framework for the performance comparison of TSN real-time scheduling methods. "+" denotes the pairing of generated workload and topology as the algorithm input.

errors in safety-critical networked applications through the integration of automotive functional safety engineering with TSN routing and scheduling. Craciunas et al. [46] propose an out-of-sync schedule robustness for TSNs that can handle synchronization failures at run time.

IV. EXPERIMENTAL SETUP

We now present the details of our experiment setup to evaluate the performance of 16 scheduling methods (see Fig. 6).

A. Hardware-based Measurements

To validate the effectiveness and practicability of existing TSN scheduling methods, we conduct an empirical study by setting up a testbed consisting of 8 bridge and 8 ESs in a ring topology as shown in Fig. 7(a). The bridge uses the COTS TTTech TSN Evaluation board for implementation, and the ES is implemented using the Linux Ethernet stack with an external Network Interface Controller (NIC).

As mentioned in Section II, most existing TAS-based scheduling methods assume that the processing delay, propagation delay, and synchronization error are constant or bounded in their system models. To the best of our knowledge, however, there is no existing work validates these assumptions through experimental measurements in real-world TSN testbeds.

We first measure the propagation delay via the round-trip time (RTT) between the directly connected talker and listener using the hardware timestamping function supported by the NIC. Fig. 7(b) shows that the propagation delay in one hop is bounded between $2ns$ and $6ns$, with a $4ns$ jitter due to the measurement inaccuracy. For the processing delay on the TTTech Evaluation board, since we cannot measure it directly, we estimate its upper bound by observing the end-to-end delay. We gradually increase the potential upper bound of the

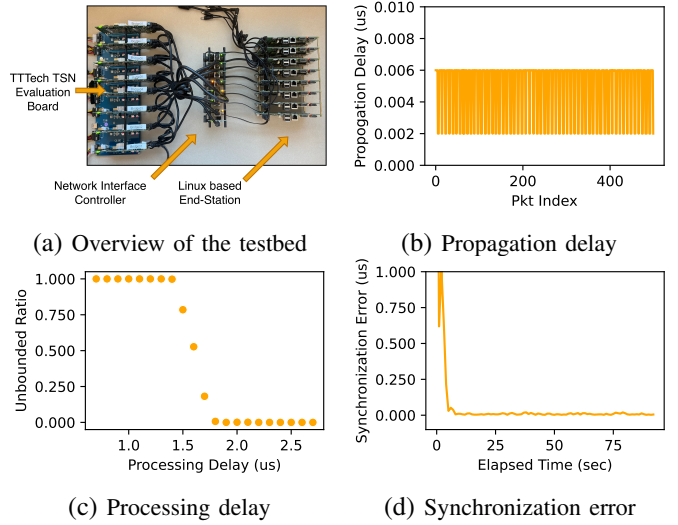


Fig. 7. Overview of the TSN testbed and the measurement results of propagation delay, processing delay and synchronization errors.

processing delay in the TAS configuration until all frames' end-to-end delay can be bounded. Fig. 7(c) shows that the processing delay at one hop can be bounded within $1.9\mu s$ in our testbed. Figure. 7(d) shows the synchronization error measured on the testbed which is reported by the logs of Linux PTP stack. It can be observed that the synchronization error converged after around 5 seconds which is caused by the grand master clock election process [47]. The synchronization error then becomes stable and bounded within $10ns$. Based on these measurement results, we set the propagation delay, processing delay and synchronization error to $6ns$, $1.9\mu s$ and $10ns$, respectively, for our subsequent experiments.

B. Workload Generation

To perform comprehensive evaluation on the performance of the scheduling methods, we vary a rich set of experimental parameters, including system utilization, number of streams, periodicity pattern, data size, and deadline, to generate diverse traffic workloads. The range of these parameter values are based on the specifications of the IEC/IEEE 60802 TSN

TABLE II
PARAMETER SETTINGS FOR THE PERFORMANCE EVALUATION.
PARAMETERS MARKED WITH * CORRESPOND TO NETWORK
SETTINGS, WHILE OTHERS REPRESENT WORKLOAD SETTINGS.

	Setting	Specification
System utilization	-	{5, 10, 15, ..., 35, 40%}
Number of streams	-	{8, 18, 28, ..., 178, 188}
Periodicity	Sparse single	{2 ms}
	Dense single	{0.4 ms}
	Sparse harmonic	{0.5, 1, 2, 4 ms}
	Dense harmonic	{0.1, 0.2, 0.4, 0.8 ms}
	Sparse inharmonic	{0.25, 0.5, 1.25, 2.5, 4 ms}
	Dense inharmonic	{0.05, 0.1, 0.25, 0.5, 0.8 ms}
Data size	Tiny size	50 bytes
	Small size	50 to 500 bytes
	Medium size	200 to 1500 bytes
	Large size	500 to 4500 bytes
	Huge size	1500 to 4500 bytes
Deadline	Implicit deadline	Period
	Relaxed deadline	NW + {0.1, 0.2, 0.4, 0.8, 1.6 ms}
	Normal deadline	NW + {0.01, 0.025, 0.05, 0.1, 0.2, 0.4 ms}
	Strict deadline	NW + {0, 0.01, 0.02, 0.025, 0.05 ms}
	No-wait deadline	NW
*Topology	Linear	8 to 98 bridges
	Ring	8 to 98 bridges
	Tree	8 to 98 bridges
	Mesh	8 to 98 bridges
*Number of queues	-	{1, 2, 3, ..., 7, 8 queues}
*Line rate	-	{10, 100, 1000 Mbps}

industrial use case [34] and the requirements of IEEE 802.1DP TSN aerospace profile [48] to ensure that our experiments can simulate representative real-world TSN applications. The workload parameter settings are summarized in Table II.

System utilization. When a set of streams are deployed in a TSN network, we define the system utilization as the average egress bandwidth utilization among all the talkers in the network. Specifically, the bandwidth utilization for each egress link is calculated as the average of each stream's data size/(period \times line rate), including all streams traversing the link. According to the worst-case system utilization commonly observed in the aerospace profile, we set the upper bound of the system utilization to 40% [48], while ensuring that the maximum bandwidth utilization of each talker is no larger than 75% as recommended in [49].

Number of streams. According to [11], most existing studies on TSN real-time scheduling assume that the number of streams is no larger than 100 in their experimental setup. In our experiments, we set the upper bound of the number of streams in a TSN network to 188, given that the real-world Orion CEV network contains 187 streams [50].

Periodicity. In our experiments, we set the period of a stream in the range of $[50\mu s, 4ms]$, which is compliant with the industrial profile's definition for isochronous traffic [34]. Based on the selected period values, we created 6 settings, namely "sparse single", "dense single", "sparse harmonic", "dense harmonic", "sparse inharmonic", and "dense inharmonic", based on if the selected periods for the stream set are constant, harmonic or arbitrary. A scenario is 'dense' if the selected period(s) are smaller while a sparse scenario has larger periods for the streams. Readers are referred to Table II for the detail.

Data size. According to the IEEE 802.1Qbv standard, one instance of a stream can be composed of multiple frame segments when the data size is larger than the MTU. The

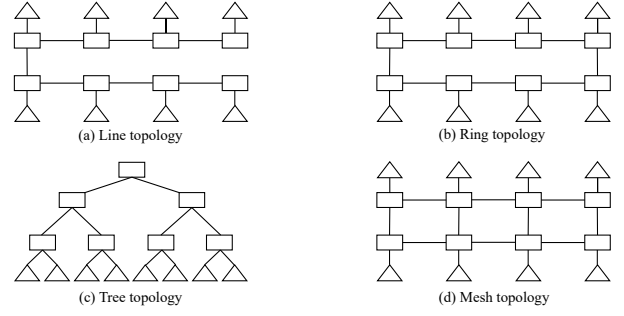


Fig. 8. Four network topologies evaluated in the experiments.

data size of a stream is defined as the sum of all segments' lengths. In the experiments, we used the MTU size for default fragmentation, and created 5 data size settings, namely 'tiny' (50 bytes), 'small' (50-500 bytes), 'medium' (200-1500 bytes), 'large' (500-4500 bytes) and 'huge' (1500-4500 bytes).

Deadline. To avoid the situation that a set of streams cannot be scheduled even when their queuing delays are all zero, we set the no-wait delay (i.e., the sum of propagation, processing and transmission delay along the shortest path) as the minimum deadline for each stream respectively. We created five different deadline settings, namely 'implicit deadline', 'relaxed deadline', 'normal deadline', 'strict deadline' and 'no-wait deadline' to progressively tighten the deadline constraints.

C. Network Settings

To evaluate the impact of network-related parameters on the performance of the scheduling methods, we further vary a set of important network parameters, including network topology, network scale, and the number of queues and line rate of each bridge. Their settings are summarized in Table II.

Network topology and scale. As shown in Fig. 8, we employ four commonly used network topologies in our experiments, namely linear, ring, tree, and mesh. The network scale is characterized by the number of bridges in the network, which is up to 98 for each topology in our experiments.

Number of queues and line rate. In our experiments, the number of available queues on each bridge is varied from 1 to 8 and the line rate of each link is selected among 10Mbps, 100Mbps and 1Gbps to evaluate their impact on the performance of the scheduling methods. Unless specifically stated, 1Gbps line rate is employed in our experiments, as gigabit bridges are most commonly used in industrial applications and offered by most vendors [51].

D. Algorithm Implementation

In this paper, we reproduced 16 existing scheduling methods as summarized in Table I. We implemented their algorithms in Python3, as some work rely on third-party software and all those software provide interface in Python3. Specifically, for SMT/OMT-based methods, we use Z3 solver to support a wide range of required theories and logical formulas such as array and arithmetic theory [52]. For ILP-based methods, we use Gurobi optimizer which is one of the most advanced ILP

solvers [53]. One exception is for JRS-NW-L, we used the CPLEX ILP solver to implement the logical indicator [54]. In addition, We employed the IBM CP Optimizer for CP-WA, following selection in the original paper. For I-ILP, we used the SpectralClustering function from the Sklearn library to implement its graph-based stream set partition algorithm [55].

It is worth noting that we made some selection and modification on some methods in our implementation to either make the evaluation practical or balance the efficiency and schedulability. We summarize those changes below.

SMT-WA. This work proposed and compared both frame- and stream-based isolation models, showing that the frame-based approach can enhance schedulability with a marginal increase (up to 13%) on the runtime. For this reason, we only implemented the frame-based isolation model to show the best schedulability it can achieve.

JRS-NW-L/JRS-MC. The model generation optimization techniques proposed in JRS-NW-L and JRS-MC are found to be counter-effective by the recent research study [20]. We thus omit them in our implementation to reduce the execution time and improve schedulability.

SMT-NW. The optimal solution in SMT-NW was implemented with the no-wait model as it showed better overall performance in our evaluation.

LS-TB. The “global conflict set” data structure used in the paper is only necessary to maintain the completeness of the algorithm, and it is only used in about 0.96% of the problem instances [24]. Thus in our implementation, we omit it to speed up and enhance the overall schedulability.

LS. The FINDIT function in LS is not explained in detail. We thus chose to implement the FINDIT function by a binary search-based strategy.

SMT-FR. We only implemented the optimal method for SMT-FR, as the proposed fixed-priority scheduling method involves worst-case delay analysis, and is difficult to implement.

CP-WA/LS-TB. We omitted the presence variable, a decision variable used to reject streams in CP-WA and LS-TB. In our evaluation, we consider a set of streams to be feasible only if they can all meet their deadlines.

I-OMT. In the OMT-based algorithms, the time validity constraint is modified by adding an indicator variable to guarantee that one frame can only be mapped to one window. We made this simplification because the original formulation was too complex and would take over 12 hours to add the constraints even for small-scale problem based on our evaluation.

For methods requiring user input parameters, we follow the default settings in their papers. For instance, we set the maximum number of windows to 5 for AT, the maximum fragment count to 5 for SMT-FR, the maximum iteration number to 100 for I-ILP, the maximum preemption count to 5 for SMT-PR, and assume a release point at 0 for all streams in LS-TB. Finally, as suggested by the IEEE 802.1Qcc standard [36], we applied the shortest path routing algorithm to construct the routes for each stream in FRS-based methods.

TABLE III
EVALUATION METRICS FOR COMPARING THE PERFORMANCE OF THE REAL-TIME SCHEDULING METHODS IN TSN.

Metric	Explanation
Schedulable ratio	Portion of feasible stream sets with computational limitation
Running time	Total duration of the algorithm's running until termination
Memory usage	Peak memory usage termination of algorithm until termination
GCL length	Maximum GCL length across all links
Overall delay & jitter	Average end-to-end delay and jitter across all streams
Link utilization	Maximum bandwidth utilized on links across all links
Queue utilization	Maximum number of utilized queues across all links
Reliability*	Robustness to meet traffic characters when faults occur
Integrity*	Correctness of payload information protected during faults

E. Evaluation Environment

Our experiments were conducted on Chameleon cloud, an NSF-sponsored public cloud computing platform [56]. We utilized 8 nodes equipped with 2x AMD EPYC® CPUs, 64 cores per CPU with a clock speed of 2.45 GHz, and 256 GB DDR4 memory. The operating system was Ubuntu 20.04 LTS. To make the benchmark robust and representative, we ran a total of 256 problem instances under each workload and network setting, with 64 experiments running simultaneously on a single node at any given time. To avoid any interference among experiments, we dedicated each experiment on a single process with a maximum of 4GB RAM and 4 threads for algorithms that support concurrency. To be practical, we constrained the maximum runtime of each algorithm to be 2 hours in the evaluation as most of the methods take less than 2 hours according to our evaluation. It is worth noting that all the evaluated algorithms in this paper aimed to generate an offline communication configuration (e.g., routes and schedules), thus a 2-hour runtime limit is acceptable. If any thread of the algorithm exceeds the time threshold, the algorithm is terminated, ‘unknown’ is returned as the result. It should be noted that certain heuristic algorithms and SMT-based algorithms may not fully utilize the 4 threads allocated, due to their lack of parallel computing support. We fixed the random seeds to 1024.

F. Evaluation Metrics

Based on the research objectives and application scenarios discussed in Section II and Section III, we summarize the commonly used evaluation metrics in Table III. Since we do not consider fault scenarios in this work, we mainly focus on the first six metrics in our performance evaluation.

V. PERFORMANCE COMPARISON

In this section, we present a comprehensive performance comparison among the 16 scheduling methods studied in this paper. We organized the experimental results according to the evaluation metrics summarized in Table III.

A. Schedulability Ratio

We first compare the schedulability ratio among all the scheduling methods with varied workload under different network settings. When a scheduling method is applied on a problem instance, it will yield one of the three results below:

- **Feasible:** A valid schedule can be constructed with the specified runtime and memory constraints.
- **Infeasible:** The stream set is not schedulable under this scheduling method, i.e., a valid schedule does not exist.
- **Unknown:** The scheduling method cannot determine if the stream set is schedulable or not with the specified runtime and memory constraints.

Assume that a scheduling method \mathcal{M} is applied to a set of problem instances \mathcal{N} generated under a given workload and network setting \mathcal{S} . Out of these $|\mathcal{N}|$ problem instances in \mathcal{N} , N_F are feasible, N_I are infeasible and N_U are unknown, and we have $N_F + N_I + N_U = |\mathcal{N}|$. Based on these results, we define the best-case and worst-case schedulability ratios of \mathcal{M} when applied to \mathcal{N} to be $SR_{\mathcal{M}}^U$ and $SR_{\mathcal{M}}^L$, by assuming that all the unknown problem instances are schedulable and unschedulable, respectively. Specifically, we have:

$$SR_{\mathcal{M}}^U = 1 - \left(\frac{N_I}{|\mathcal{N}|}\right) \quad \text{and} \quad SR_{\mathcal{M}}^L = \frac{N_F}{|\mathcal{N}|} \quad (1)$$

The key design rationale behind these two schedulability ratios is to fairly estimate the best and worst ability of a scheduling method to construct feasible schedule under a given experimental setting. By employing these two metrics as the experimental lower bound and upper bound of the schedulability ratios of \mathcal{M} , we can determine that \mathcal{M} outperforms another scheduling method \mathcal{M}' under the same experimental setting \mathcal{S} if $SR_{\mathcal{M}}^L \geq SR_{\mathcal{M}'}^U$.

To quantify the comparison between the ability of two scheduling methods \mathcal{M} and \mathcal{M}' to find valid schedules without considering the unknown cases, we further define a metric called schedulability advantage, denoted as $SA(\mathcal{M}, \mathcal{M}')$. Specifically, let $\mathcal{F}(\mathcal{M}, \mathcal{M}', i)$ be a function that returns 1 if \mathcal{M} finds a feasible solution and \mathcal{M}' returns infeasible for problem instance i , and 0 for any other cases. Let $\mathcal{G}(\mathcal{M}, \mathcal{M}', i)$ be another function that returns 1 if both \mathcal{M} and \mathcal{M}' return feasible or infeasible results for problem instance i , and 0 otherwise. $SA(\mathcal{M}, \mathcal{M}')$ can be defined as follows:

$$SA(\mathcal{M}, \mathcal{M}') = \sum_{i=1}^N \frac{\mathcal{F}(\mathcal{M}, \mathcal{M}', i)}{\mathcal{G}(\mathcal{M}, \mathcal{M}', i)}. \quad (2)$$

We say that method \mathcal{M} strictly outperforms method \mathcal{M}' when applied to problem set \mathcal{N} under the same experimental setting \mathcal{S} if $SA(\mathcal{M}, \mathcal{M}') > SA(\mathcal{M}', \mathcal{M}) = 0$.

1) *Overall Trends:* With these definitions, in the first set of the experiments, we evaluate how the system utilization and network scale will impact the schedulability ratio of individual methods, and the results are summarized in Fig. 9. Each experiment randomly selects the periodicity, data size, deadline, and topology settings from Table II, while having the number of available queues set to 8 and the line rate set to 1Gbps. Fig. 9(a) and Fig. 9(b) demonstrate the performance of $SR_{\mathcal{M}}^U$ and $SR_{\mathcal{M}}^L$ for each scheduling method \mathcal{M} , respectively, along with the increase of the system utilization. In the

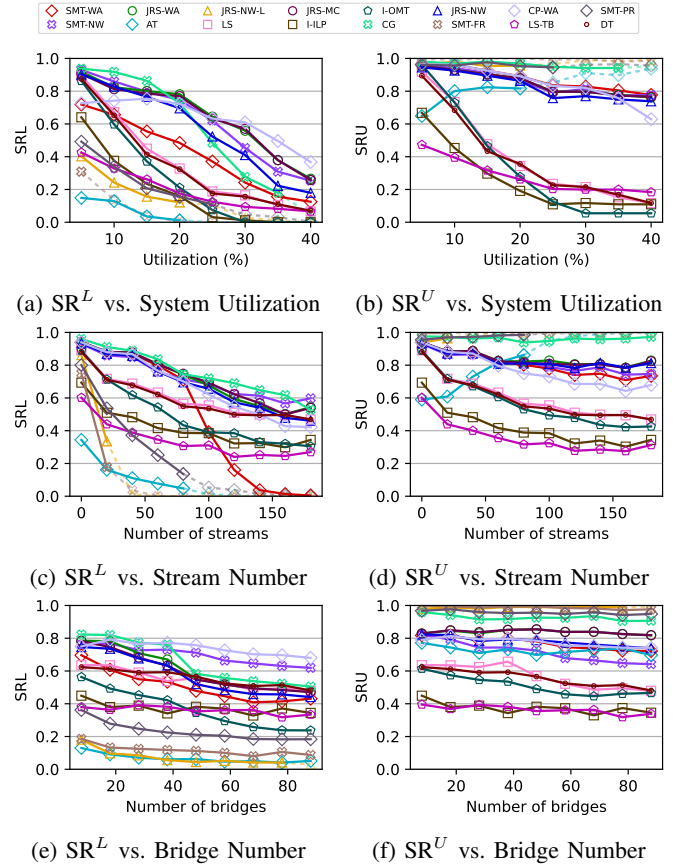


Fig. 9. Comparison of the schedulability ratios with varied workload and network scale (number of streams and bridges).

experiments, system utilization was increased from 5% to 40% by randomly adding streams until the expected utilization was met, with the number of bridges held constant at eight. Fig. 9(c) and Fig. 9(d) demonstrate the performance of the schedulability ratios along with the increase of the number of streams deployed in the TSN network. In the experiments, the number of streams is varied from 8 to 188, with 8 bridges in the network and randomly selected utilization. Fig. 9(e) and Fig. 9(f) further demonstrate the performance of the schedulability ratios along with the increase of the number of bridges in the TSN network. In the experiments, the number of bridges is varied from 8 to 88, with randomly selected utilization and number of streams. In the results, we use the dashed lines and transparent nodes to represent data points which have over 95% unknown results, which may not be of statistical significance to conclude on the method's schedulability under those specific settings.

From this set of experiments, we can clearly observe that $SR_{\mathcal{M}}^L$ of each method \mathcal{M} consistently decreases along with the increase of the system utilization and the number of streams deployed in the network. Figure 9(a) and Figure 9(c) show that the overall SR^L decreases from 69.3% to 10.6% when the system utilization increases from 5% to 40%, and the average SR^L of all methods decreases from 58.7% to 31.0% when the number of streams increases from 8 to 188. From Figure 9(b)

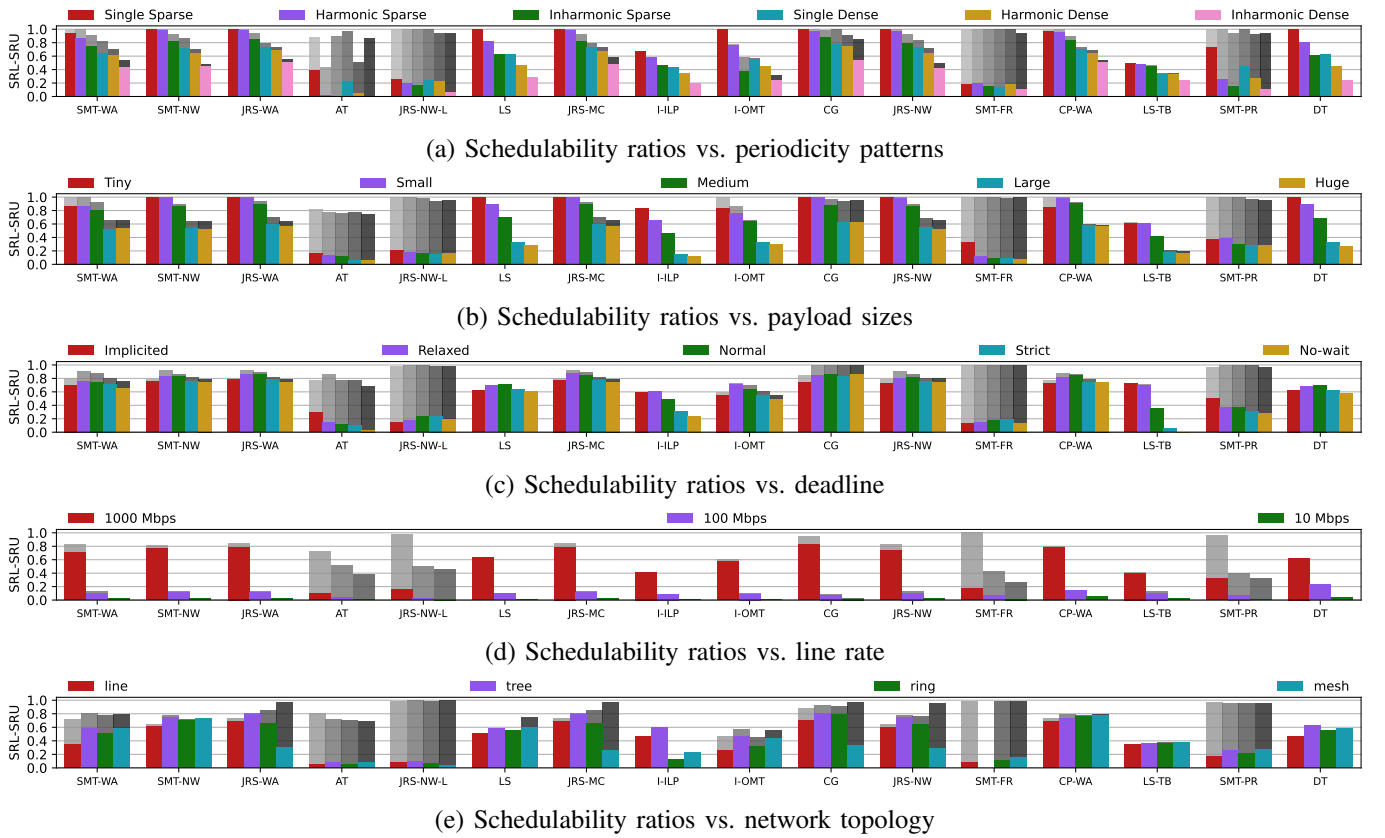


Fig. 10. Comparison of the schedulability ratios among the scheduling methods with varied stream and network specifications.

and Figure 9(d), some moderate performance degradation of SR^U can also be observed. For example, the overall SR^U decreases from 88.7% to 61.6% along with the increase of the system utilization, and from 89.8% to 72.6% when the number of streams in the network is increased from 8 to 188. Interestingly, Figure 9(e) and Figure 9(f) show that increasing the number of bridges in the network doesn't have significant impact on the schedulability ratios of individual methods. For example, the overall SR^L and SR^U slightly decrease from 55.3% to 36.5% and 76.9% to 69.5%, respectively, when the number of bridges are increased from 8 to 88. A possible reason for this observation is that while a network with more bridges typically yields more links and longer routing paths, making the scheduling problem more complex, it also provides more routing paths and reduces the flow collisions, thereby expanding the solution space.

Based on the results in Fig. 9, we have the following finding:

Finding (1): The increase of workload poses a significant challenge to scheduling the stream set in a TSN network, whereas the increase of network scale has little impact on the schedulability with our experimental settings.

In the second set of experiments, we evaluate the impact of specific stream and network specifications on the schedulability ratios of different methods. Our results are summarized in Fig. 10. We randomly select the system utilization, number of streams, and number of bridges in each experiment, while

having the number of available queues set to 8. Fig. 10(a) compares all 16 methods' $SR^U_{\mathcal{M}}$ and $SR^L_{\mathcal{M}}$ across 6 different periodicity patterns, while randomly selecting the payload size, deadline, and topology with a constant 1Gbps line rate. Similarly, Fig. 10(b)-(e) shows how the schedulability ratios change with varied settings on payload size, deadline, line rate and network topology while other parameters are randomly selected. We use the grey bars to represent SR^U values, while the colorful areas are used to represent SR^L . Each group of bars summarizes the results for one scheduling method.

From Fig. 10(a), we can clearly observe that a stream set with smaller periods (dense setting) and more arbitrary period patterns (inharmonic setting) usually has lower schedulability ratios. For example, stream sets with denser periodicity exhibit lower average SR^L from 67.4% to 43.8% and SR^U values from 88.7% to 67.0% compared to those with sparser periodicity. Furthermore, the SR^L decreased from 66.8% to 57.3% to 42.7%, and SR^U also decreased from 86.0% to 76.8% and further to 69.4% for the single, harmonic, and inharmonic periodicity cases, respectively. Fig. 10(b) shows that larger payload sizes lead to lower schedulability ratios for all the methods. Specifically, by increasing the payload size from 'tiny' to 'huge' setting, we find that the average SR^L of all the methods decrease from 75.4% to 35.4%, and SR^U decreases from 95.5% to 56.0%. Fig. 10(c) shows that extending the deadlines of the streams only yields limited benefits on improving the schedulability ratios for most of

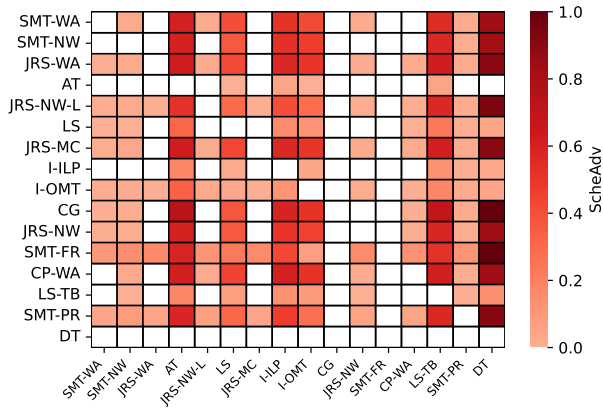


Fig. 11. Pairwise schedulability comparison among the 16 methods.

methods, due to the fact that our experiment settings force the stream's no-wait delay to be less than its deadline. The results in Fig. 10(d) follow our expectation that the decrease of the line rate substantially reduces both SR^L and SR^U for all the studied methods, with SR^L at 54.9%, 9.7%, and 1.8%, and SR^U at 76.6%, 21.0%, and 10.5% for 1000/100/10Mbps line rates, respectively. By employing different topologies in Fig. 10(e), we can observe that SR^U on tree and mesh topology is slightly higher than those with line and ring topology. For instance, the mesh and tree topologies have SR^U of 76.9% and 73.8%, while that of the ring and line topologies are 79.9% and 69.1% respectively. We explain it as streams typically have fewer hops between the talker and listener on mesh and tree topology with equal network scale. Despite this, the mesh topology introduces more links, thereby expanding the scheduling problem and reducing SR^L to 37.8%, compared to the tree topology's 54.9%.

Based on results in Fig. 10, we have the following finding:

Finding (2): The parameter settings of periodicity, payload size, line rate and network topology consistently influence the schedulability ratio for most scheduling methods. The deadline setting only affects specific methods due to our workload generation.

2) *Model Comparison:* Based on the results collected from the first two sets of experiments, we can derive the pairwise schedulability advantage results and present them in a heatmap format in Fig. 11. In this heatmap, each cell represents the $SA(\mathcal{A}, \mathcal{B})$ value for method \mathcal{A} and \mathcal{B} . A darker red cell indicates a higher $SA(\mathcal{A}, \mathcal{B})$ value, meaning that the method on the row-index outperforms the method on the column-index. From Fig. 11, we have the following important observations.

First of all, our results show that the joint fragmentation and scheduling method (SMT-FR) and joint preemption and scheduling method (SMT-PR) outperform most other methods disregarding runtime and memory limitations. We define the average SA of method \mathcal{M} as $\sum_{\mathcal{M}' \neq \mathcal{M}} SA(\mathcal{M}, \mathcal{M}')$ to represent its superiority over other methods concerning SA . SMT-FR and SMT-PR show average SA values of 23.4% and 23.7%, respectively, significantly higher than other methods.

Since SA does not consider the unknown cases, it validates that incorporating fragmentation and preemption mechanisms can improve the schedulability without the computational resource limitation. This conclusion is further validated in Fig. 9 and Fig. 10, where both methods show high SR^U .

On the other hand, when taking the unknown cases into consideration, SMT-FR and SMT-PR show poor schedulability due to their increased computational overhead. Fig. 9(a)(c)(e) show that these two methods have considerably lower SR^L values compared to other methods. For example, SMT-FR exhibits notably low SR^L values as 6.1% and 10.0% with varied system utilization and number of streams, respectively. A similar result can be observed for SMT-PR, which only achieves 17.3% and 21.5% SR^L , respectively. The contrasting results between SR^U and SR^L suggest that while complex models can enhance the likelihood of finding feasible solutions in challenging scenarios that simple models deem infeasible, the efficiency trade-off from these complex models can decrease performance in the worst case due to exceeding runtime or memory limitations.

Based on above discussion, we have the following finding:

Finding (3): While models based on fragmentation and preemption can significantly enhance schedulability, they may become counterproductive when the computational resources are limited.

Another important observation from Fig. 11 is that JRS-based methods can significantly improve their schedulability ratio on topologies with routing capabilities (e.g., ring and mesh) without considering computational resource limitations. We first compare four wait-allowed models: JRS-WA, JRS-MC, CP-WA, and SMT-WA. From the pairwise comparison in Fig. 11, JRS-WA and JRS-MC strictly outperform CP-WA and SMT-WA in terms of SA values. In addition, by comparing the absolute schedulability values, Fig. 10(e) shows that JRS-WA and JRS-MC outperforms SMT-WA and CP-WA on SR^U in ring (with two routes) and mesh topology (with \geq two routes), and no significant difference for line and tree topology (with only one route). Similar outcomes can also be observed in no-wait based methods between JRS-NW and SMT-NW.

Nevertheless, JRS-based methods suffer from high computational overhead and lead to lower schedulability with runtime and memory limitations. From Fig. 9(e), we notice that the SR^L of JRS-WA significantly decreases when transitioning from line (68.5%) and tree (78.6%) topologies to ring (65.5%) and mesh (30.3%) topologies, underperforming compared to SMT-WA and CP-WA on identical topology settings. Similar trends can be observed in JRS-MC and JRS-NW as well. Moreover, integrating heuristic algorithms can mitigate the loss in schedulability caused by computational overhead. For example, the LS method, a JRS-based heuristic approach, only shows a minor drop in SR^L values, from 50.3% and 58.9% in line and tree topologies respectively, to 55.6% and 50.3% in ring and mesh topologies as shown in Fig. 9(e). Thereby, we

have the following finding:

Finding (4): Joint routing and scheduling can enhance schedulability on multi-path topology. However, it requires optimization to carefully manage the algorithm's computational complexity.

Unfortunately, by comparing the no-wait and wait-allowed models, no consistent superiority can be found on the schedulability. We first compare two FRS-based methods SMT-NW and SMT-WA. From the results in Fig. 11, SMT-WA strictly outperforms SMT-NW on SA as expected due to its more flexible delay model. However, from the absolute schedulability ratios, there is no evidence that SMT-WA consistently outperforms SMT-NW on SR^L or SR^U . Then we compare JRS-based methods JRS-NW and JRS-WA. Fig. 11 shows that JRS-WA strictly outperforms JRS-NW on SA as expected. However, there is also no consistent comparison results between the two methods. For example, in Fig. 9(a)(c), we can only observe that JRS-WA significantly outperforms JRS-NW in terms of SR^L when the system utilization is large than 20%, and when the number of streams is larger than or equal to 78. In addition, JRS-WA exhibits better SR^U only when the number of bridges is greater than 28.

Our results also reveal that the window-based scheduling method, AT, has poor values on both SR^U and SR^L and is outperformed by most of the other methods on SA . This is because the schedulability of AT is highly sensitive to the algorithm input (number of maximum windows), and inadequate number of allowed windows will lead to infeasible results under the settings with large workload. In addition, its schedulability heavily depends on the available computing resources due to the large design space from the combination of window allocation and frame-to-window mapping. By replacing the constraint on the number of windows as the objective function and incorporating heuristic decomposition into the model, the I-OMT method effectively addresses the above issues, thereby improving SR^U , SR^L , and SA .

3) *Exact vs. Heuristic Solutions*: Fig 9 shows that exact solutions clearly outperform the heuristic approaches in both SR^L and SR^U as system utilization and number of streams varies. For SR^L , from Fig. 9(a)(c), we can observe that the exact solutions (JRS-WA, CP-WA, SMT-NW, JRS-NW, and JRS-MC) yield significantly better results compared to the heuristic approaches (I-OMT, LS, I-ILP, LS-TB, DS). The performance of the heuristic approaches show a sharp decrease along with the increase of the system utilization, and ultimately fall below an average 10% SR^L when the utilization reaches 40%. On the other hand, these heuristic approaches exhibit slower decrease when the number of streams in the network increases, and two of them (LS and DT) even have similar SR^L compared to those of some exact solutions when the number of streams exceeds 148. Regarding to SR^U , Fig. 9(b)(d) show that the exact solutions consistently dominate heuristic approaches. For the SA values, Fig. 11 shows that five heuristic approaches

(LS, I-ILP, I-OMT, LS-TB, DT) have significant higher values in the column, indicating that they are outperformed by most other methods on SA and their schedulability is also lower than exact solutions without considering the unknown cases.

Based on above discussion, we have the following finding:

Finding (5): Exact solutions can achieve higher schedulability and no heuristic approach can achieve a comparable performance.

4) *Comparison of Individual Methods*: We have shown that the variations of experimental setup (e.g., changes of network topology or workload) may have different impact on the schedulability of different scheduling methods, and may lead to unexpected results that contradict with their original design considering the computational resource limitation. We now show that some methods can have inconsistent comparison results under varied experiment settings:

- CG outperforms other methods on SR^L when the system utilization $< 15\%$. However, its SR^L drops quickly and becomes worse than other exact solutions when the system utilization keeps increasing (see Fig. 9(a)).
- CP-WA has comparably lower performance compared to other exact solutions on SR^L . It outperforms others when the system utilization is large than 30% (see Fig. 9(a)). This is because of the high scalability introduced by the CP formalization.
- SMT-WA has similar performance compared to other exact solutions on SR^L in the beginning. However, it drops quickly when the number of streams is large than 100 (see Fig. 9(c)) due to exceed memory limitation.
- SMT-NW shows lower SR^L compared with CG when the number of bridges is less than 48. However, the performance of CG decreases quickly along with the increase of number of bridges in the network (see Fig 9(e)).
- I-OMT has higher SR^L compared to SMT-WA (99.6% vs. 94.1%) under the single and sparse period setting. However, SMT-WA shows higher SR^L under all other periodicity settings because I-OMT is shown to have poor schedulability with inharmonic stream set in Fig. 10(a). This is because the algorithm is sensitive to the Least Common Multiple (LCM) of the stream set's period, where inharmonic stream sets usually result in a larger LCM.
- DT has better SR^L (100%) compared with SMT-WA (86.3%) under the tiny payload setting. However, it can be observed that SMT-WA can achieve both higher SR^U and SR^L under other periodicity settings in Fig. 10(b).
- LS-TB has higher SR^L and SR^U in the experiments with implicit and relaxed deadline settings than DT. However, LS-TB shows significantly lower SR^L and SR^U when the deadline constraint is tight because its searching space is restricted to the relative deadline length in Fig. 10(e).

Based on above discussion, we have the following finding:

Finding (6): Achieving a fair comparison among all the scheduling methods is challenging and different experimental settings can lead to even opposite conclusions.

We also notice some unexpected results for each individual method. In Fig. 10(e), we notice that I-ILP has poor performance on both SR^U and SR^L in both ring and mesh topologies compared with line and tree. This might imply that the heuristic Doc-Aware routing algorithm proposed in the paper may be counter-effective, as other JRS-based methods can usually achieve higher SR^U on multi-path topology.

Our last finding is that using logical formalization within ILP might not be effective on schedulability. Even though JRS-NW-L and JRS-NW are using the same system model, JRS-NW has significantly better performance than JRS-NW-L on both SR^U and SR^L . This maybe because JRS-NW-L utilizes the logical indicator constraint, which may have weaker relaxations during the ILP optimization, a condition that can lead to more computational effort in a model [57].

B. Runtime

In this section, we compare the computational efficiency of the scheduling methods by measuring their algorithm runtime under different settings. This critical performance metric evaluates how well the scheduling algorithm will scale [49].

In the first set of the experiments, we evaluate how the system utilization, network scale and topology will impact the runtime of individual methods, and the results are summarized in Fig. 12. In our experiments, the runtime of a scheduling algorithm consists of the pre-processing time (filtering the invalid solution space), the constraint adding time, and the problem solving time. Note that, if the scheduling method incorporates an objective function, we only measure its runtime to find a feasible solution, rather than the optimal one, to avoid an unfair comparison among methods that have an additional focus on schedule quality.

1) *Overall Trends:* Fig. 12 shows the algorithm runtime as a function of the system utilization, the number of streams, and the number of bridges (in both single-path topology and multi-path topology settings). Each experiment randomly assigns periodicity, data size, deadline and topology parameters according to the settings in Table. II, with the number of available queues set to 8 and the line rate set to 1Gbps. Fig. 12(a)-(d) show the runtime of each method \mathcal{M} as we increase the system utilization, stream numbers, bridge numbers in single-path topology (line and tree), and bridge numbers in multi-path topology (ring and mesh).

From the results, we can clearly observe that increasing the workload (system utilization and number of streams) will significantly increase the runtime of all the methods. For instance, as shown in Fig. 12(a), the overall runtime of all the evaluated methods increases from 15.7 to 40.1 minutes when the system utilization increases from 5% to 45%. Fig. 12(b) shows that the overall runtime increases from 2.66 to 33.21 minutes when the number of streams increases from 8 to 188.

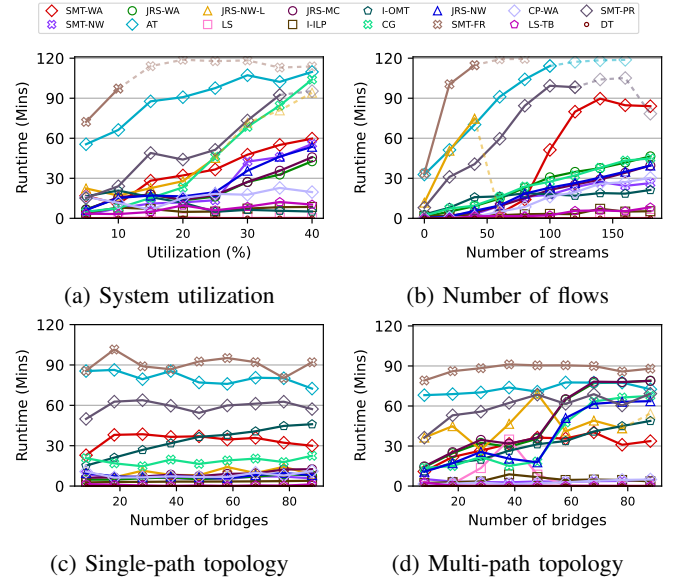


Fig. 12. Comparison of the algorithm runtime with varied workload, network scale and topology.

Interestingly, increasing the number of bridges in the network does not significantly impact the runtime. Fig. 12(c) shows that the overall runtime increases from 16.69 to 18.64 minutes when the network scales up from 8 to 88 bridges in both line and tree topologies. This is because a larger network scale does not automatically lead to a larger problem scale (i.e., an increase in decision variables or number of constraints). For instance, in the case of the no-wait-based FRS model, the number of decision variables solely depends on the number of streams. This disconnection between network scale and runtime is also observed in [17], [20]. Fig. 12(d) shows that only seven methods (SMT-WA, JRS-WA, JRS-MC, JRS-NW, I-OMT, CG, and SMT-PR) exhibit runtime increase from 17.82 to 36.94 minutes. This modest increase in runtime can be attributed to commonly used preprocessing techniques such as path reduction and path cut-off, as seen in methods like JRS-WA, JRS-MC, and JRS-NW. By path reduction, these methods scale with the subgraphs created by the paths of the streams, rather than the original topology.

Based on Fig. 12, we have the following finding:

Finding (7): The runtime increases with system utilization and number of streams, while the network scale changes may not have a significant impact on runtime.

We further evaluate the variation of algorithm runtime against five parameters: periodicity, payload size, deadline, number of queues, and line rate. The results are summarized in Table IV. When we vary one selected parameter, the remaining parameters are selected randomly for each problem instance. For the first three experiments, we set the number of queues to 8 and set the line rate to 1Gbps.

Table IV shows that scheduling methods typically require a longer runtime for stream sets with dense periods. Specifically,

TABLE IV
COMPARISON OF RUNTIME AND MEMORY CONSUMPTION UNDER
DIFFERENT WORKLOAD AND NETWORK SPECIFICATIONS.

	Setting	Solving time	Runtime	Memory
period	Harmonic Dense	13.07	15.57	464.06
	Harmonic Sparse	11.20	12.44	434.06
	Inharmonic Dense	8.23	17.57	563.62
	Inharmonic Sparse	10.27	17.69	554.47
	Single Dense	19.93	22.28	485.38
	Single Sparse	12.80	12.97	380.37
payload	Huge	16.08	20.33	537.49
	Large	16.41	20.70	518.11
	Medium	13.55	15.82	477.91
	Small	11.74	14.68	477.13
	Tiny	9.81	13.76	446.03
	Implicit	11.59	14.34	458.74
deadline	No-wait	13.95	17.29	487.65
	Normal	13.57	16.85	479.09
	Relaxed	14.07	17.95	515.87
	Strict	12.34	15.77	465.81
	Multiple queue	12.82	16.50	483.05
	Single queue	13.00	15.96	453.88
rate	10 Mbps	3.20	5.14	352.55
	100 Mbps	5.58	7.47	370.82
	1000 Mbps	11.94	15.30	494.75

under the harmonic settings, the average runtime increases from 12.44 to 15.57 minutes as we move from 'Sparse' to 'Dense', and under the single settings, the average runtime increases from 12.97 to 22.28 minutes. The change under the inharmonic setting is minimal, with a slight decrease from 17.69 to 17.57 minutes. However, there is no significant trend in average runtime for the single, harmonic, and inharmonic settings. Furthermore, the results also show that increasing the payload size from tiny to huge increases the average runtime from 13.76 to 20.33 minutes, implying that the payload size is also a major contributor to the algorithm runtime. However, according to Table IV, there is no clear evidence that varying the stream deadlines or the available number of queues significantly impacts the runtime. Regarding the line rate, we find that it takes longer runtime on 1Gbps networks than that on 100/10 Mbps networks. To better understand the above findings, we remove the unknown results for each method and only summarize the runtime for their feasible and infeasible results in Fig. 13. The results indicate that most methods, except AT and SMT-PR, require more time to find a feasible solution. This may explain why 10/100 Mbps and inharmonic dense networks are not as time-consuming as expected, given their low SR^L as discussed in Section V-A.

2) *Model Comparison*: As expected, we observe that models with extra features such as window-based, fragmentation, and preemption typically experience runtime growth faster when the workload increases (see Fig. 12(a)(b)). That is, models supporting fragmentation, preemption, limited GCL are less scalable compared to other methods along as the workload increases. For instance, SMT-FR quickly reaches the runtime limit at 20% system utilization or over 40 streams, while SMT-PR's average runtime exceeds 90 minutes when the system utilization is greater than 35% and the number of streams is larger than 100. In addition, window-based method AT shows larger runtime when compared to other methods,

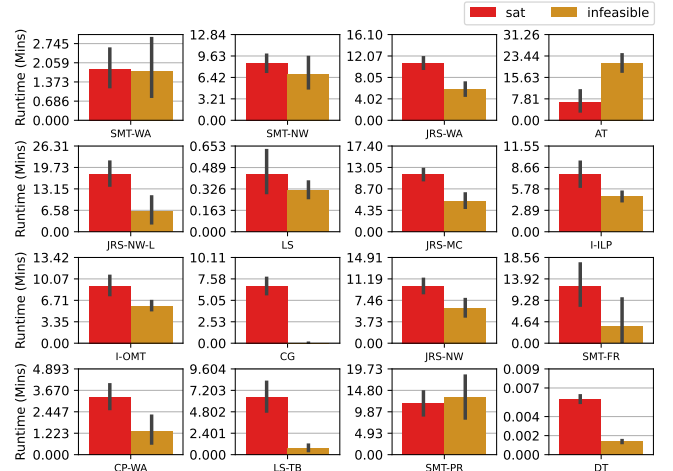


Fig. 13. Average runtime: feasible cases vs. infeasible cases.

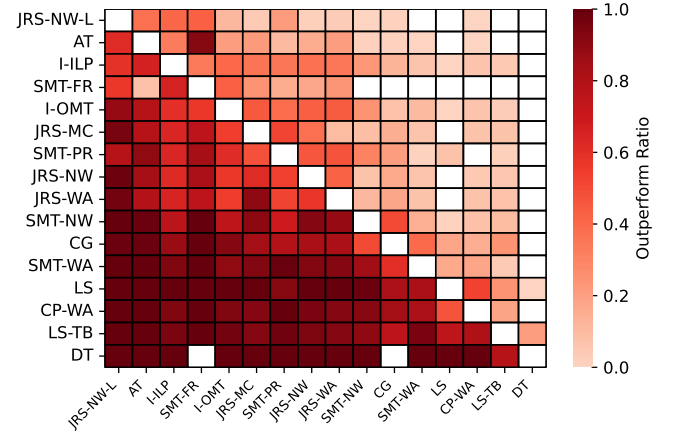


Fig. 14. Pairwise overall runtime comparison among the 16 methods.

remaining the second worst across all experiments in Fig. 12.

We also discover that JRS models are more sensitive to the change of the network scale in ring and mesh topologies. As depicted in Fig. 12(d), the runtime of JRS-MC experiences a substantial increase from an average of 14.75 minutes to 78.83 minutes when the number of bridges increases from 8 to 88. In a similar way, JRS-WA has its runtime increased from 14.22 minutes to 78.99 minutes. Both methods employ the wait-allowed JRS model. In addition, two no-wait JRS methods, CG and JRS-NW, show that the runtime increases from 13.61 to 47.54 minutes and 10.76 to 63.62 minutes by increasing the number of bridges from 8 to 88. Interestingly, JRS-NW-L and LS show a trend of increasing runtime before decreasing, reaching their peak values when there are 50 and 40 bridges in the network, respectively. For FRS models, most methods exhibit no significant changes in runtime when the number of bridges is increased. However, I-OMT, an FRS-based method, shows an increased runtime in line and tree topology along with the increased number of bridges. This may be due to the fact that as a window-based method, the number of links in I-OMT increases along with the increased number of bridges

and thus introduce more decision variables into the problem.

Another interesting observation is that employing logical formalization in ILP or SMT can result in rapid growth of runtime as the number of streams increases. This can be observed from the growth rates of three logical formalization methods, I-OMT, JRS-NW-L, and SMT-WA in Fig.12(b), which are notably faster compared to Fig. 12(a). On the other hand, the collision graph based method has similar runtime growth rate compared to other no-wait JRS-based methods when the number of streams increases. But it is not scalable along with the increase of the system utilization, quickly reaching its time limit when the system utilization is 40%.

From the above discussion, we have the following finding:

Finding (8): Different scheduling models exhibit diverse runtime patterns under different settings. This suggests that a general solution might not exist for handling the diverse factors that contribute to the runtime growth.

3) *Algorithm Comparison*: In Fig.14, we present a pairwise comparison of the overall runtime among all scheduling methods, considering only their feasible or infeasible results (i.e., excluding the unknown ones). We say that method *A* strictly outperforms *B* in terms of runtime, if for all the problem instances that *A* and *B* generate the same results, *A* is always faster. For instance, from the results in Fig. 14, we observe that SMT-WA strictly outperforms JRS-NW-L since SMT-WA is faster than JRS-NW-L on solving all the problem instances when they generate the same results.

From Fig. 14, we can observe that heuristic methods DT, LS, and LS-TB outperform most exact solutions in terms of runtime. The FRS-based method DT, which employs divisibility theory, demonstrates the best performance, strictly outper CP-WA, SMT-WA, JRS-WA, SMT-PR, JRS-MS, and JRS-NW-L). This can also be confirmed in Fig. 12, where DT maintains a runtime below three seconds across all the workload and network scale settings. Similarly, the JRS-based method LS shows low runtime due to its list scheduler, outperforming exact solutions such as JRS-WA, JRS-NW, JRS-MC, and JRS-NW-L on runtime. Its runtime remains consistently below one minute under various workload and network settings in our experiments as shown in Fig.12(a)(b)(c), although it has slightly increased runtime in multi-path topologies as shown in Fig. 12(d). The other FRS-based method using list scheduler, LS-TB, also shows similar performance. Finally, heuristic methods based on iterative optimization, such as I-OMT and I-ILP, substantially reduce the runtime compared to the exact solutions under the same models. Specifically, I-OMT outperforms AT in 98.6% of the problem instances, and I-ILP outperforms JRS-NW in 59.8% of the problem instances according to Fig. 14. The low runtime of the above two heuristic approaches is also confirmed in Fig. 12.

Based on the above analysis, we have the following finding:

Finding (9): Heuristic approaches designed to improve scalability can significantly reduce the runtime compared to exact solutions.

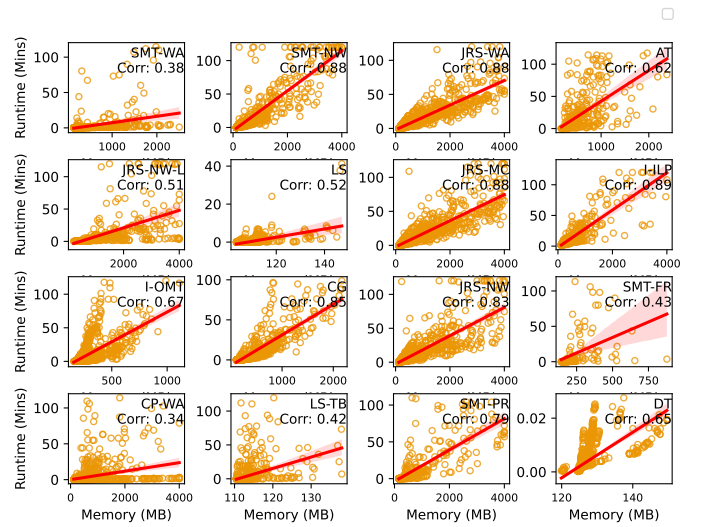


Fig. 15. The correlation between algorithm runtime and memory consumption with unknown results excluded.

Finally, in addition to heuristic approaches, we also confirm that the proposed techniques for improving scalability, such as CP-based and conflict-graph-based solutions, are also effective on reducing the algorithm runtime. For instance, under the same scheduling model but employing a constraint programming (CP)-based implementation, CP-WA outperforms SMT-WA in 81.7% of the problem instances in Fig. 14. CP-WA also shows better scalability along with the increase of the system utilization and number of streams as shown in Fig. 12(a)(b). Furthermore, by mapping the problem onto a conflict graph, CG demonstrates great scalability. It outperforms SMT-NW, an ILP-based solution under the same model. Even though CG has long runtime in some cases such as under high system utilization and large-scale multi-path network settings, it can still achieve a good trade-off and high schedulability.

C. Memory Consumption

In the third set of experiments, we compare the scalability of various scheduling methods regarding their memory consumption. According to the IEEE 802.1QCC standard, a centralized network configuration (CNC) device manages multiple functions such as scheduling, path allocation, and bridge configuration [36]. Given that the CNC device is typically an embedded system with limited memory and processing resource, it is important for the scheduling methods to have small memory footprint especially when the network scales up. In our evaluation, we measure the peak memory usage for each method. We set the memory limit at 4GB to ensure sufficient RAM is available and to prevent the usage of swapping space. The memory usage is reported by the Linux kernel and recorded during the full course of the algorithm execution.

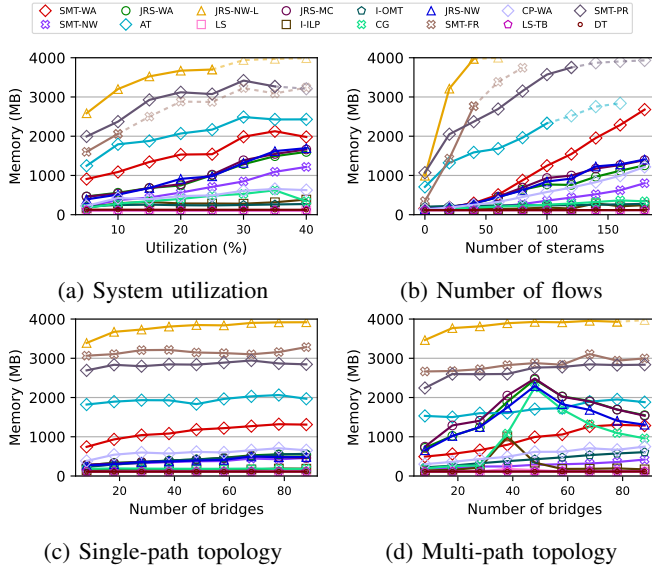


Fig. 16. Comparison of the memory consumption with varied workload, network scale and topology.

Fig. 15 shows the correlation between the algorithm runtime and memory consumption for each scheduling method, without including the unknown results. In practice, high correlation implies that optimizing either runtime or memory consumption could result in the improvement of the other performance. On the other hand, low correlation suggests certain bottlenecks, requiring the optimization of memory consumption or runtime to be performed separately. In addition, Fig. 16 demonstrates how the memory consumption changes along with the increased system utilization, number of flows, and number of bridges under different topologies.

From Fig. 15, we can observe that methods with a correlation above 0.8 are all ILP-based methods utilizing the big-M formalization. In contrast, methods with logical and all-different formalizations show much lower correlation, indicating that their memory consumptions are not aligned with their computational overhead. We also find that SMT-WA, JRS-NW-L, and CP-WA methods experience significant memory consumption bottlenecks. This is evidenced by many instances in Fig. 15 which show large memory consumption but low algorithm runtime. These observations are also confirmed by the results shown in Fig. 16. On the other hand, the AT, CG, and I-OMT methods demonstrate opposite behaviors with low memory consumption but large runtime overhead. For instance, although CG's runtime increases rapidly as shown in Fig. 12(a)(b) with the increase of the system utilization and the number of streams, compared to other no-wait scheduling models (e.g., SMT-NW), CG exhibits great scalability in terms of memory consumption, as shown in Fig. 16(a)(b).

Finding (10): Memory consumption is correlated with runtime for most of the scheduling methods. Instances of non-correlation may suggest specific bottlenecks.

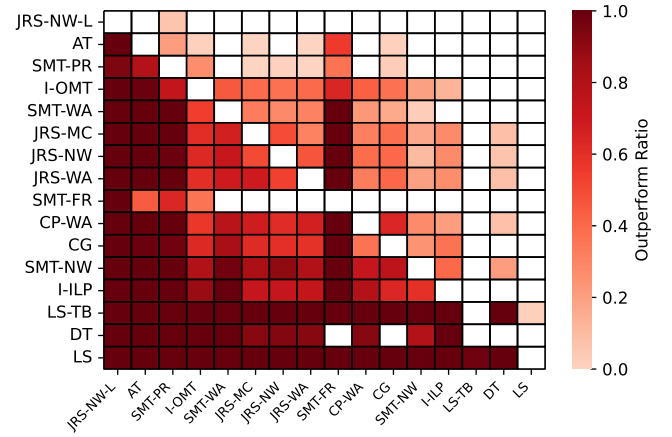


Fig. 17. Pairwise memory comparison among the 16 methods.

Fig. 17 introduces the memory advantage metric (similar to the runtime advantage metric introduced in Section V-B) to quantify the relative memory consumption performance among different methods. This performance metric excludes the unknown results but focuses only on the problem instances where two methods return either feasible or infeasible results. We say A strictly outperforms B if A consistently consumes less memory than B when they have the same output. From Fig. 17, we can observe that LS, LS-TB, DT, and I-ILP demonstrate very high memory efficiency, and LS and LS-TB strictly outperform most of the other methods. Fig. 17 demonstrates that models incorporating additional features, such as JRS, JFS, JPS, and window-based methods exhibit larger memory consumption compared to other methods. This is mainly because these models typically require more decision variables to calculate factors such as routing paths, preemptive classes and fragmentation sizes.

Finding (11): Most proposed approaches for improving scalability can also reduce the overall memory, while models with additional features usually lead to higher memory consumption.

Fig. 18 summarizes the percentage of unknown results due to either the memory and runtime limits. We observe from the results that the factors leading the scheduling methods to return unknown results vary significantly. For example, the logical-based formulations (e.g., SMT-WA, AT, JRS-NW-L, and SMT-FR) mainly generate unknown results due to memory limitations. In contrast, methods using linear formulations tend to be terminated due to both the memory and runtime limits when using ILP solvers. CP formulations and heuristic algorithms are typically terminated due to runtime limits.

D. Other Metrics

In addition to schedulability and scalability (in terms of runtime and memory consumption), which describe the effectiveness and efficiency of the scheduling methods in finding feasible solutions, the quality of the solution (i.e., the gener-

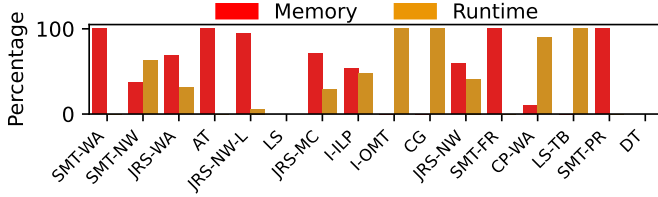


Fig. 18. Percentage of problem instances terminated with unknown results caused by either memory or runtime limit.

ated schedule) is also crucial. In this section, we evaluate the solution quality of the scheduling methods in terms of GCL length, overall end-to-end delay and jitter of the schedule, link utilization, and queue utilization.

1) *GCL Length*: Fig. 19 shows the distribution of the maximum GCL length used by each scheduling method in our evaluation. The statistical results summarized herein are derived from all experiments conducted in previous sections. The distribution plot was generated using the kernel density estimates method [58], and the average of the distribution is provided in the top-right corner. Please note that in the experiments, we only can discuss schedule quality for the problem instances that can be solved by the scheduling methods, and each method has a different number of solved instances due to their varied schedulability.

From Fig. 19, it can be observed that AT, being a window-based method, has an extremely low average GCL length (four entries), reflecting the strict constraint of a maximum of five windows per link in our settings. I-OMT, another window-based method aiming to minimize the number of GCL entries, has an average of 81 maximum entries, which is still low compared to the other methods. SMT-PR has a low average maximum GCL length of 19, which can be attributed to the overlapping entries during preemption. Nevertheless, some frame-based methods without GCL length constraints may exceed 2000 entries in certain scenarios, in contrast to the typical maximum GCL length for TSN bridges, which ranges from 8 to 1024 [18].

2) *Overall End-to-End Delay & Jitter*: Fig. 20 presents the average end-to-end delay for all streams across each method, varying with workload and network scale. It can be observed from Figure.20(a) that no-wait based methods maintain almost constant delay when the system utilization increases. For the wait-allowed model, we observe that JRS-NW-L, CP-WA, and LS-TB exhibit consistently growing delay along with the increase of the system utilization, while the end-to-end delays in other methods fluctuate. Fig. 20(b) shows similar observation with increased number of bridges in the network. Moreover, Fig. 20(b) also reveals that JRS-based wait-allowed models tend to have larger end-to-end delay compared to the FRS-based models when the bridge number increases.

In Figure. 20(c)(d), we evaluate the jitter of the constructed schedules by increasing the number of streams and bridges in the network, respectively. The results show that only AT,

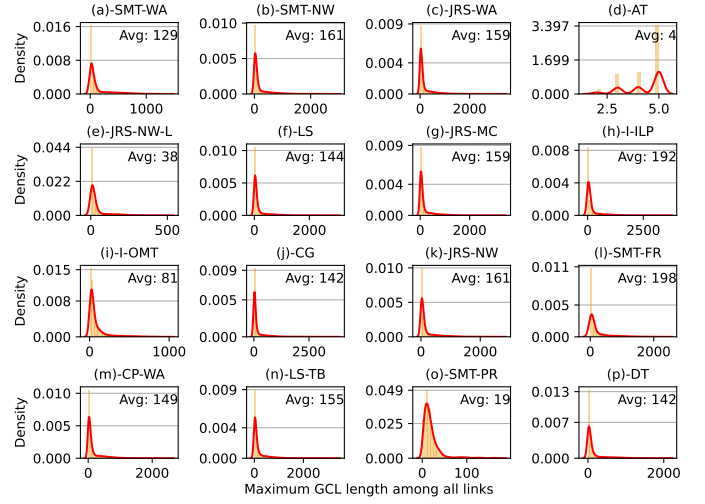


Fig. 19. Distribution of the maximum GCL length among all the solvable problem instances for each method.

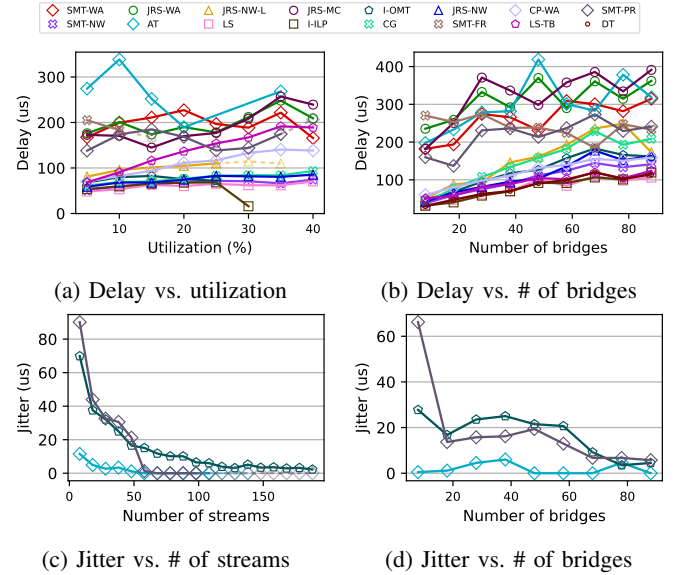


Fig. 20. Comparison of the end-to-end delay and jitter with varied workload and topology.

I-OMT, and SMT-PR follow the jitter-allowed model, while the other methods follow the no-jitter model; thus, we omit the other methods as they exhibit zero jitter. Interestingly, from the results we observe a decrease of the jitter when more streams or bridges are added into the network.

3) *Link Utilization*: Fig. 21 shows the distribution of the peak link utilization among all the solvable problem instances for each scheduling method. As seen in Fig. 21, the distribution forms a long tail for most scheduling methods, except for I-OMT. Although the average peak link utilization for all methods is below 21%, the tail of the distribution can surpass 75% utilization in specific scenarios. This suggests that certain scenarios may leave inadequate bandwidth for other traffic classes, underscoring the importance of reducing

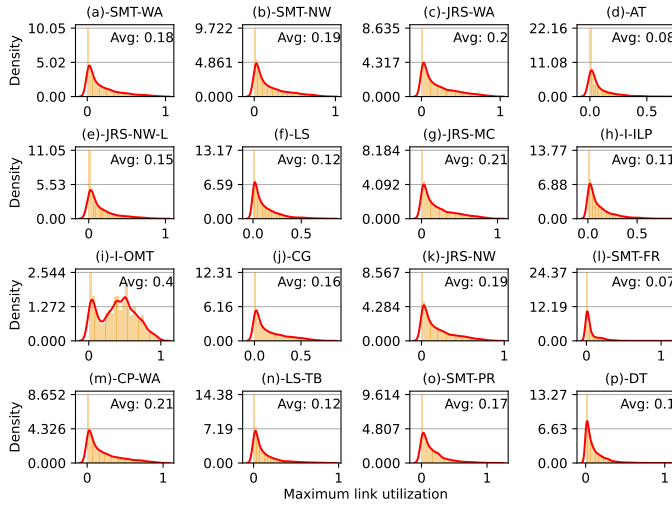


Fig. 21. Distribution of the maximum link utilization among all solvable problem instances for each method.

the bandwidth of TT traffic. We also observe that I-OMT, as a window-based method, tends to over-allocate resources during the scheduling, as it has a noticeably higher average link utilization of 40% compared to other methods.

4) *Queue Utilization*: Fig.22 shows the distribution of the maximum queue utilization across all solvable problem instances for each method. No-wait based models (SMT-NW, JRS-NW-L, LS, I-ILP, CG, JRS-NW, and SMT-FR) use only one queue, while wait-allowed methods (SMT-WA, AT, I-OMT, CP-WA, and LS-TB) with explicit queuing can have a maximum of 8 queues in our experimental settings. It is important to note that due to the omission of queuing assignment, we modified methods with implicit queuing models such as JRS-WA, JRS-MC and SMT-PR, by assigning each stream to a dedicated queue on each hop, ensuring the FIFO property. However, this post-processing strategy may result in the average queue utilization to easily surpass the total number of available queues on the bridge.

VI. CONCLUSIONS AND FUTURE WORK

The growing interest in TSN aims to achieve ultra-low latency and deterministic communications over switched Ethernet networks. This paper examines 16 state-of-the-art real-time scheduling methods based on Time-aware Shaper (TAS) and establishes a benchmark for performance evaluation using various metrics. Comprehensive experiments are conducted to compare these algorithms, highlighting their strengths and weaknesses in various scenarios. This paper aims to assist researchers in identifying the current state and open problems in TSN scheduling algorithm design, offering insight towards future TSN research and development.

As the future work, we will enhance our simulation results by incorporating realistic problem instances from avionic and automobile industries, as well as increasing the evaluation scale with additional problem instances. To further evaluate the

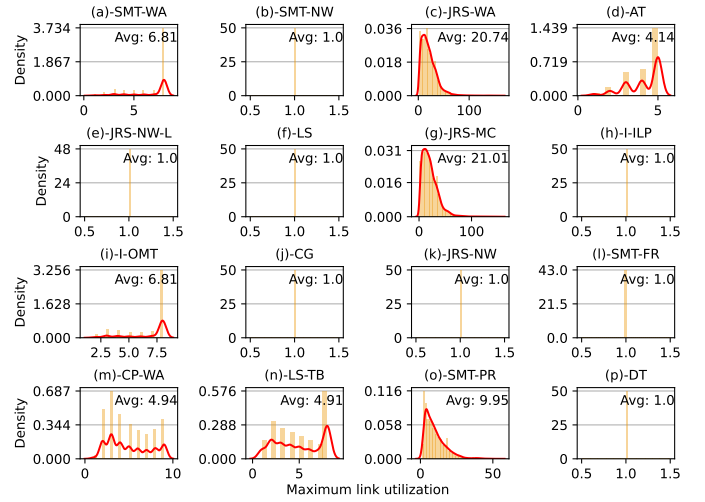


Fig. 22. Distribution of the maximum queue utilization among all solvable problem instances for each method.

correctness and practicability of the existing TAS scheduling methods, we will conduct more comprehensive empirical experiments on our TSN testbed. Finally, we will open source our benchmark's dataset and source code to the community to boost TSN-related research and development projects.

VII. ACKNOWLEDGEMENT

The work is supported in part by the National Science Foundation Grant CNS-1932480, CNS-2008463, CCF-2028875, CNS-1925706, and the NASA RETHi project.

REFERENCES

- [1] E. Sisinni, A. Saifullah, S. Han, U. Jennehag, and M. Gidlund, "Industrial internet of things: Challenges, opportunities, and directions," *IEEE transactions on industrial informatics*, vol. 14, no. 11, pp. 4724–4734, 2018.
- [2] W. Z. Khan, M. Rehman, H. M. Zangoti, M. K. Afzal, N. Armi, and K. Salah, "Industrial internet of things: Recent advances, enabling technologies and open challenges," *Computers & Electrical Engineering*, vol. 81, p. 106522, 2020.
- [3] "Ieee standard for local and metropolitan area networks– virtual bridged local area networks amendment 12: Forwarding and queuing enhancements for time-sensitive streams," *IEEE Std 802.1Qav-2009*, pp. 1–72, 2010.
- [4] "Ieee standard for local and metropolitan area networks–bridges and bridged networks - amendment 34:asynchronous traffic shaping," *IEEE Std 802.1Qcr-2020*, pp. 1–151, 2020.
- [5] "Ieee standard for local and metropolitan area networks–bridges and bridged networks–amendment 29: Cyclic queuing and forwarding," *IEEE 802.1Qch-2017*, pp. 1–30, 2017.
- [6] "Ieee standard for local and metropolitan area networks – bridges and bridged networks - amendment 25: Enhancements for scheduled traffic," *IEEE Std 802.1Qbv-2015*, pp. 1–57, 2016.
- [7] L. Zhao, P. Pop, and S. Steinhorst, "Quantitative performance comparison of various traffic shapers in time-sensitive networking," *IEEE Transactions on Network and Service Management*, vol. 19, no. 3, pp. 2899–2928, 2022.
- [8] D. Hellmanns, J. Falk, A. Glavackij, R. Hummen, S. Kehrler, and F. Dürr, "On the performance of stream-based, class-based time-aware shaping and frame preemption in tsn," in *2020 IEEE International Conference on Industrial Technology (ICIT)*. IEEE, 2020, pp. 298–303.

- [9] H. Kopetz, A. Ademaj, P. Grillinger, and K. Steinhammer, "The time-triggered ethernet (tte) design," in *Eighth IEEE International Symposium on Object-Oriented Real-Time Distributed Computing (ISORC'05)*. IEEE, 2005, pp. 22–33.
- [10] Y. Lin, X. Jin, T. Zhang, M. Han, N. Guan, and Q. Deng, "Queue assignment for fixed-priority real-time flows in time-sensitive networks: Hardness and algorithm," *Journal of Systems Architecture*, vol. 116, p. 102141, 2021.
- [11] T. Stüber, L. Osswald, S. Lindner, and M. Menth, "A survey of scheduling in time-sensitive networking (tsn)," *arXiv preprint arXiv:2211.10954*, 2022.
- [12] A. Minaeva and Z. Hanzálek, "Survey on periodic scheduling for time-triggered hard real-time systems," *ACM Computing Surveys (CSUR)*, vol. 54, no. 1, pp. 1–32, 2021.
- [13] L. Deng, G. Xie, H. Liu, Y. Han, R. Li, and K. Li, "A survey of real-time ethernet modeling and design methodologies: From avb to tsn," *ACM Computing Surveys (CSUR)*, vol. 55, no. 2, pp. 1–36, 2022.
- [14] A. Nasrallah, A. S. Thyagaturu, Z. Alharbi, C. Wang, X. Shao, M. Reisslein, and H. ElBakoury, "Ultra-low latency (ull) networks: The ieee tsn and ietf detnet standards and related 5g ull research," *IEEE Communications Surveys & Tutorials*, vol. 21, no. 1, pp. 88–145, 2018.
- [15] Y. Seol, D. Hyeon, J. Min, M. Kim, and J. Paek, "Timely survey of time-sensitive networking: Past and future directions," *IEEE Access*, vol. 9, pp. 142 506–142 527, 2021.
- [16] A. Nasrallah, V. Balasubramanian, A. Thyagaturu, M. Reisslein, and H. ElBakoury, "Tsn algorithms for large scale networks: A survey and conceptual comparison," *arXiv preprint arXiv:1905.08478*, 2019.
- [17] S. S. Craciunas, R. S. Oliver, M. Chmélík, and W. Steiner, "Scheduling real-time communication in ieee 802.1 qbv time sensitive networks," in *Proceedings of the 24th International Conference on Real-Time Networks and Systems*, 2016, pp. 183–192.
- [18] R. S. Oliver, S. S. Craciunas, and W. Steiner, "Ieee 802.1 qbv gate control list synthesis using array theory encoding," in *2018 IEEE Real-Time and Embedded Technology and Applications Symposium (RTAS)*. IEEE, 2018, pp. 13–24.
- [19] E. Schweissguth, P. Danielis, D. Timmermann, H. Parzyjegl, and G. Mühl, "Ilp-based joint routing and scheduling for time-triggered networks," in *Proceedings of the 25th International Conference on Real-Time Networks and Systems*, 2017, pp. 8–17.
- [20] D. Hellmanns, L. Haug, M. Hildebrand, F. Dürr, S. Kehrer, and R. Hummen, "How to optimize joint routing and scheduling models for tsn using integer linear programming," in *29th International Conference on Real-Time Networks and Systems*, 2021, pp. 100–111.
- [21] J. Falk, F. Dürr, and K. Rothermel, "Exploring practical limitations of joint routing and scheduling for tsn with ilp," in *2018 IEEE 24th International Conference on Embedded and Real-Time Computing Systems and Applications (RTCSA)*. IEEE, 2018, pp. 136–146.
- [22] E. Schweissguth, D. Timmermann, H. Parzyjegl, P. Danielis, and G. Mühl, "Ilp-based routing and scheduling of multicast realtime traffic in time-sensitive networks," in *2020 IEEE 26th International Conference on Embedded and Real-Time Computing Systems and Applications (RTCSA)*. IEEE, 2020, pp. 1–11.
- [23] F. Dürr and N. G. Nayak, "No-wait packet scheduling for ieee time-sensitive networks (tsn)," in *Proceedings of the 24th International Conference on Real-Time Networks and Systems*, 2016, pp. 203–212.
- [24] M. Vlk, K. Brejchová, Z. Hanzálek, and S. Tang, "Large-scale periodic scheduling in time-sensitive networks," *Computers & Operations Research*, vol. 137, p. 105512, 2022.
- [25] M. Pahlevan, N. Tabassam, and R. Obermaier, "Heuristic list scheduler for time triggered traffic in time sensitive networks," *ACM Sigbed Review*, vol. 16, no. 1, pp. 15–20, 2019.
- [26] X. Jin, C. Xia, N. Guan, and P. Zeng, "Joint algorithm of message fragmentation and no-wait scheduling for time-sensitive networks," *IEEE/CAA Journal of Automatica Sinica*, vol. 8, no. 2, pp. 478–490, 2021.
- [27] A. A. Atallah, G. B. Hamad, and O. A. Mohamed, "Routing and scheduling of time-triggered traffic in time-sensitive networks," *IEEE Transactions on Industrial Informatics*, vol. 16, no. 7, pp. 4525–4534, 2019.
- [28] M. Vlk, Z. Hanzálek, and S. Tang, "Constraint programming approaches to joint routing and scheduling in time-sensitive networks," *Computers & Industrial Engineering*, vol. 157, p. 107317, 2021.
- [29] X. Jin, C. Xia, N. Guan, C. Xu, D. Li, Y. Yin, and P. Zeng, "Real-time scheduling of massive data in time sensitive networks with a limited number of schedule entries," *IEEE Access*, vol. 8, pp. 6751–6767, 2020.
- [30] Y. Zhou, S. Samii, P. Eles, and Z. Peng, "Time-triggered scheduling for time-sensitive networking with preemption," in *2022 27th Asia and South Pacific Design Automation Conference (ASP-DAC)*. IEEE, 2022, pp. 262–267.
- [31] J. Falk, F. Dürr, and K. Rothermel, "Time-triggered traffic planning for data networks with conflict graphs," in *2020 IEEE Real-Time and Embedded Technology and Applications Symposium (RTAS)*. IEEE, 2020, pp. 124–136.
- [32] J. Zou, M. Eiselt, M. Alfageme, J. Agusti, C. Teres, P. Ciria, R. Veisllari, M. Fontaine, and J.-P. Elbers, "Recent trials of g. metro-based passive wdm fronthaul in 5g testbeds," in *2019 IEEE International Conference on Communications Workshops (ICC Workshops)*. IEEE, 2019, pp. 1–6.
- [33] I. S. Association et al., "Ieee standard for local and metropolitan area network—bridges and bridged networks," *IEEE Std 802.1 Q-2018 (Revision of IEEE Std 802.1 Q-2014)*, pp. 1–1993, 2018.
- [34] J. Dorr, K. Weber, and S. Zuponic, *Use Cases IEC/IEEE 60802*. [Online]. Available: <https://www.ieee802.org/1/files/public/docs2018/60802-industrial-use-cases-0918-v13.pdf>
- [35] L. Zhao, P. Pop, Z. Zheng, and Q. Li, "Timing analysis of avb traffic in tsn networks using network calculus," in *2018 IEEE Real-Time and Embedded Technology and Applications Symposium (RTAS)*. IEEE, 2018, pp. 25–36.
- [36] "Ieee standard for local and metropolitan area networks—bridges and bridged networks—amendment 31: stream reservation protocol (srp) enhancements and performance improvements," *IEEE Std 802.1 Qcc-2018*, 2018.
- [37] A. Mascis and D. Pacciarelli, "Job-shop scheduling with blocking and no-wait constraints," *European Journal of Operational Research*, vol. 143, no. 3, pp. 498–517, 2002.
- [38] Y. Zhang, Q. Xu, S. Wang, Y. Chen, L. Xu, and C. Chen, "Scalable no-wait scheduling with flow-aware model conversion in time-sensitive networking," in *GLOBECOM 2022-2022 IEEE Global Communications Conference*. IEEE, 2022, pp. 413–418.
- [39] IEEE, "Ieee standard for local and metropolitan area networks—bridges and bridged networks—amendment 26: frame preemption: 802.1 qbu-2016," 2016.
- [40] R. Mahfouzi, A. Aminifar, S. Samii, P. Eles, and Z. Peng, "Security-aware routing and scheduling for control applications on ethernet tsn networks," *ACM Transactions on Design Automation of Electronic Systems (TODAES)*, vol. 25, no. 1, pp. 1–26, 2019.
- [41] X. Dai, S. Zhao, Y. Jiang, X. Jiao, X. S. Hu, and W. Chang, "Fixed-priority scheduling and controller co-design for time-sensitive networks," in *Proceedings of the 39th International Conference on Computer-Aided Design*, 2020, pp. 1–9.
- [42] M. Barzegaran, B. Zarrin, and P. Pop, "Quality-of-control-aware scheduling of communication in tsn-based fog computing platforms using constraint programming," in *2nd Workshop on Fog Computing and the IoT (Fog-IoT 2020)*. Schloss Dagstuhl-Leibniz-Zentrum für Informatik, 2020.
- [43] B. Houtan, M. Ashjaei, M. Daneshmand, M. Sjödin, and S. Mubeen, "Synthesising schedules to improve qos of best-effort traffic in tsn networks," in *29th International Conference on Real-Time Networks and Systems*, 2021, pp. 68–77.
- [44] N. Reusch, P. Pop, and S. Craciunas, "Technical report: Safe and secure configuration synthesis for tsn-based distributed cyber-physical systems using constraint programming," 2020.
- [45] Y. Zhou, S. Samii, P. Eles, and Z. Peng, "Asil-decomposition based routing and scheduling in safety-critical time-sensitive networking," in *2021 IEEE 27th Real-Time and Embedded Technology and Applications Symposium (RTAS)*. IEEE, 2021, pp. 184–195.
- [46] S. S. Craciunas and R. S. Oliver, "Out-of-sync schedule robustness for time-sensitive networks," in *2021 17th IEEE International Conference on Factory Communication Systems (WFCS)*. IEEE, 2021, pp. 75–82.
- [47] "Ieee standard for local and metropolitan area networks—timing and synchronization for time-sensitive applications," *IEEE Std 802.1AS-2020*, pp. 1–421, 2020.
- [48] W. Fischer, J. Gelish, and M. Hegarty, *Aerospace tsn use cases, traffic types, and requirements*. [Online]. Available: <https://www.ieee802.org/1/files/public/docs2021/dp-Jabbar-et-al-Aerospace-Use-Cases-0321-v06.pdf>

- [49] D. Pannell, "Choosing the right tsn tools to meet a bounded latency," *IEEE SA Ethernet & IP@ Automotive Technology Day*, 2019.
- [50] D. Tămaş-Selicean, P. Pop, and W. Steiner, "Design optimization of tternet-based distributed real-time systems," *Real-Time Systems*, vol. 51, pp. 1–35, 2015.
- [51] D. Bruckner, R. Blair, M. Stanica, A. Ademaj, W. Skeffington, D. Kutscher, S. Schriegel, R. Wilmes, K. Wachswender, L. Leurs *et al.*, "Opc ua tsn," *A new Solution for Industrial Communication*, 2019.
- [52] L. De Moura and N. Bjørner, "Z3: An efficient smt solver," in *Tools and Algorithms for the Construction and Analysis of Systems: 14th International Conference, TACAS 2008, Held as Part of the Joint European Conferences on Theory and Practice of Software, ETAPS 2008, Budapest, Hungary, March 29-April 6, 2008. Proceedings 14*. Springer, 2008, pp. 337–340.
- [53] L. Gurobi Optimization, "Gurobi optimizer reference manual," 2021.
- [54] T. Manuals, "Cplex document," 2019.
- [55] F. Pedregosa, G. Varoquaux, A. Gramfort, V. Michel, B. Thirion, O. Grisel, M. Blondel, P. Prettenhofer, R. Weiss, V. Dubourg *et al.*, "Scikit-learn: Machine learning in python," *the Journal of machine Learning research*, vol. 12, pp. 2825–2830, 2011.
- [56] K. Keahey, J. Anderson, Z. Zhen, P. Riteau, P. Ruth, D. Stanzione, M. Cevik, J. Colleran, H. S. Gunawi, C. Hammock, J. Mambretti, A. Barnes, F. Halbach, A. Rocha, and J. Stubbs, "Lessons learned from the chameleon testbed," in *Proceedings of the 2020 USENIX Annual Technical Conference (USENIX ATC '20)*. USENIX Association, July 2020.
- [57] P. A. Rubin, "Perils of "big m"," Jul 2011. [Online]. Available: <https://orinanobworld.blogspot.com/2011/07/perils-of-big-m.html>
- [58] B. W. Silverman, "Using kernel density estimates to investigate multimodality," *Journal of the Royal Statistical Society: Series B (Methodological)*, vol. 43, no. 1, pp. 97–99, 1981.